SCULPTOR Has Your Back(up Path): Carving Interdomain Routes to Services

Paper #156, 12 pages body, **TBD: 19** pages total

Abstract

Large cloud/content (service) providers serve an expanding suite of applications that are increasingly integrated with our lives, but have to contend with a dynamic public Internet to route user traffic. To enhance reliability to dynamic events such as failure and DDoS attacks, Service Providers overprovision to accommodate peak loads and activate emergency systems for shifting excess traffic. We take a different approach with SCULPTOR, which proactively advertises many prefixes for users so that Service Providers can use their global resources to meet generic objectives. SCULPTOR models Internet routing to solve a large integer optimization problem at scale using gradient descent. We prototyped SCULPTOR on a global public cloud and tested it in real Internet conditions, demonstrating that SCULPTOR handles dynamic loads 28% larger than other solutions using existing Service Provider infrastructure, reduces overloading on links during site failures by up to 40%, and enables Service Providers to route high-priority traffic with 2× less overloading.

1 Introduction

Compiled on 2024/09/19at 10:05:52

Cloud/content providers (hereafter Service Providers) enable diverse Internet applications used daily by billions of users. Traditionally, Service Providers used DNS and static BGP advertisements to define a single path from a user to a service, leaving the specific path largely up to the Internet to determine.

Increasingly, however, these services have diverse requirements that can be challenging to meet with a single path that Service Providers have little control over. For example, enterprise services have tight reliability requirements [55, 52], and new applications such as virtual reality require ≤ 10 ms round trip latency [76] and ≤ 3 ms jitter [102]. Complicating matters, Service Providers must meet these requirements subject to changing conditions such as peering link/site failures [30, 71], DDoS attacks [79, 111, 90], flash crowds [47, 60, 63], new applications/business priorities (LLMs), and route changes [77, 69, 36, 70, 84, 71]. Critically, such changes can cause *overload* if the Service Provider cannot handle new traffic volumes induced by the change, and DNS/BGP are slow mechanisms with which to change how traffic flows over paths. This overload can lead to degraded service for users, hurting reliability [78, 88, 56, 52], and may require manual intervention to remedy.

To try to meet different goals and respond to changing conditions, Service Providers adopt solutions that are either (a) too conservative, (b) too reactive, or (c) too specific. For example, Service Providers proactively overprovision resources [103, 1, 65], but we demonstrate using traces that bursty traffic patterns can require excessively conservative overprovisioning rates as high as 70% despite sufficient global capacity (§2.3). TIPSY responds to changing loads to retain reliability [71], but only does so reactively, which could lead to short-term degraded performance. AnyOpt and PAINTER proactively set up routes to optimize specific objectives such as steady-state latency [115, 55], but it is challenging to extend those approaches to other objectives (§5.4). It is also unclear both how to combine these approaches (*e.g.,* retaining low latency under changing traffic loads) and how to apply approaches from one domain to another (*e.g.,* applying egress traffic cost reduction systems [99] to ingress traffic).

We present Service Providers with a flexible framework, SCULPTOR (**S**couring **C**onfigurations for **U**tilization-**L**oss-and **P**erformance-aware **T**raffic **O**ptimization & **R**outing), which accepts as input cost, performance, and reliability objectives and outputs BGP advertisements and traffic allocations that help achieve those desired objectives. SCULPTOR is the first system that optimizes ingress interdomain routing objectives such as maximum link utilization, transit cost, and latency for *interdomain* traffic (existing systems optimize for intradomain traffic, *e.g.,* [48, 37, 72, 15]). We leave a formal characterization of the objectives, constraints, and problem sizes SCULPTOR covers to future work, and instead demonstrate its practical utility (§5). SCULPTOR computes BGP advertisements proactively, only placing live traffic on them after con-

vergence, and hence does not run the risk of outages.

To solve each optimization problem, SCULPTOR efficiently searches over the large BGP advertisement search space ($> 2^{10,000}$ possibilities) by modeling how different strategies perform, without having to predict the vast majority of actual paths taken under different configurations since predicting interdomain paths is hard and measuring them is slow (§3.3). SCULPTOR then optimizes these (modeled) performance metrics using gradient descent, which is appropriate in our setting due to the high dimension of the problem and the parallelism that gradient descent admits (§3.4). This modeling enables SCULPTOR to assess > 20M configurations (10,000× more than other solutions [115, 55]) while only measuring tens in the Internet (§5.4).

We prototype and evaluate our framework at Internet scale using the PEERING testbed [93] (§4), which is now deployed at 32 Vultr cloud locations [108]. Vultr is a global public cloud that allows our prototype to issue BGP advertisements via more than 10,000 peerings. We evaluate our framework on two specific objectives (computed separately): (a) optimizing latency under unseen traffic conditions, and (b) routing different traffic classes. We compare SCULPTOR's performance on both problems to that of an unreasonably expensive "optimal" solution (computing the actual optimal is infeasible).

For the first objective, we found that, compared to other approaches, SCULPTOR increases the amount of traffic within 10 ms of the optimal by 19.3% in steady-state (meeting that target for 95% of traffic) (§5.2.1), by 11% during link failure, and by 17% during site failure. SCULPTOR also reduces overloading on links during site failures by up to 41% over PAINTER, giving Service Providers more confidence that services will still be available during partial failure (§5.2.2). We also find that, by load balancing traffic on backup paths during peak times, we can satisfy high peak demands with the same infrastructure. SCULPTOR can handle flash crowds (*e.g.,* DDoS attacks) at more than 3× expected traffic volume, reducing the amount of overprovisioning that Service Providers need, thus reducing costs.

For the second objective, SCULPTOR routes bulk low-priority traffic in ways that avoid congesting high priority traffic, achieving near-optimal latency and reducing congestion by up to 2× (§5.3).

After decades of intradomain traffic optimization using programmable networking primitives such as virtual output queueing for differentiated service [82] (and others, §7), SCULPTOR brings such control closer to realization in the interdomain setting with no buy-in from other networks. Service Providers can use flexible frameworks such as SCULPTOR to help bring us the resilient, performant service that our diverse applications increasingly need.

2 Motivation

2.1 Variable, Evolving Goals

Evolving Internet use cases are pushing Service Providers to meet diverse requirements for their applications. For example, Service Providers increasingly host mission-critical services such as enterprise solutions [55], which require high reliability and are predicted to be a $60B industry by 2027 [46]. Gaming is a similarly important industry generating more revenue than the music and movie industries combined [5], but instead requires latency within 50 ms [76]. Service Providers are also expanding the set of services they provide—for example, CDNs that traditionally hosted static content are pivoting to offering services like compute [19, 28, 27].

Moreover, as use cases evolve, Service Providers increasingly need to meet performance requirements for *ingress* traffic since that traffic includes, for example, player movements in real-time games, voice and video in enterprise conferences, and video/image uploads for AI processing in the cloud [17, 74]. This reality is a departure from traditional CDN traffic patterns where ingress traffic was primarily small requests and TCP acknowledgments.

Despite Service Providers' efforts to meet variable service requirements [71, 51, 35, 58, 75, 55, 65], meeting requirements is still challenging due to issues *outside* Service Provider control.

First, Service Providers lack control over which ingress path traffic takes since BGP, the Internet's interdomain routing protocol, computes paths in a distributed fashion, giving each intermediate network a say in which paths are chosen and which are communicated to other networks. BGP only chooses a single path, and that path may not be the best one for meeting a given requirement. Service Providers cannot even unilaterally control the part of the path closest to them—upgrading peering capacity requires coordination among multiple parties [95].

Second, dynamic factors outside Service Provider control make satisfying requirements even harder. Peering disputes can lead to congestion on interdomain links and inflated paths [30, 21, 25], and DDoS attacks still bring down sites/services [90, 78, 88, 56], despite the considerable effort in mitigating DDoS attack effects [79, 111]. Moreover, recent work [63, 84, 15] and blog posts [47, 60, 77, 69, 36, 70] show that user traffic demands are highly variable due to flash crowds and path changes and so can be hard to plan for.

2.2 Routing Traffic to Service Providers

One way of meeting service requirements, despite this lack of control, is to (a) configure a good set of interdomain paths and (b) balance traffic on these paths to satisfy requirements. Existing systems balance traffic over egress interdomain paths [95, 114, 37, 59], but it remains unclear how to configure and

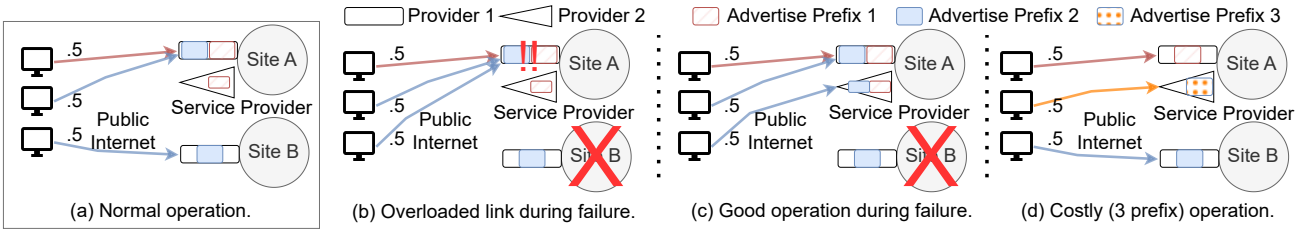

Figure 1: In normal operation traffic is split between two sites by directing half the traffic to each prefix (a). When site B fails, there is enough global capacity to serve all traffic (each link can handle 1 unit) but no way to split traffic across multiple providers given available paths leading to link overload (b). A *resilient* solution is to advertise prefix 2 to an additional provider at site A, allowing traffic splitting across the two links (c). A simpler but prohibitively expensive solution is to advertise one prefix per peering (d).

balance traffic across a good set of *ingress* interdomain paths.

Today, most Service Providers either use `anycast` prefix advertisements to provide relatively low latency and high availability at the expense of some control [8, 54, 119, 118], or `unicast` prefix advertisements to direct users to specific sites [98, 57, 95, 13].

`Anycast`, where Service Providers advertise a single prefix to all peers/providers at all sites, offers some natural availability following failures since BGP automatically reroutes most traffic to avoid the failure after tens of seconds [119]. Prior work shows that this availability comes with higher latency in some cases [64, 54]. `Unicast` gives clients lower latency than `anycast` by advertising a unique prefix at each site [98, 13], but can suffer from reliability concerns, potentially taking as much as an hour to shift traffic away from bad routes [55].

2.3 Limitations of Current Approaches

Too Specific: Recent work has similarly noted that, by offering better interdomain routes, Service Providers can achieve better performance [30, 8, 115, 118, 55]. These solutions advertise different prefixes to subsets of all peers/providers to offer users more paths. However, these solutions optimize specific objectives, mostly steady-state latency, and it is unclear how to extend their approaches to other objectives (§5.4), especially those with capacity constraints.

Figure 1 shows how this specific focus on a single objective could lead to reliability issues, *e.g.,* during a site failure. In normal operation, user traffic is split evenly across two prefixes and achieves low latency (Fig. 1a). However when site B fails, BGP chooses the route through Provider 1 for all traffic, causing link overutilization and subsequent poor performance for all users (Fig. 1b). In Section 5 we show that this overload happens in practice for state-of-the-art systems that provide low (steady-state) latency from users to Service Provider networks such as `AnyOpt` [115] and `PAINTER` [55].

Too Reactive: To enhance reliability, some Service Providers propose systems that react to changing conditions—for example, `TIPSY` drains traffic from overloaded links/sites [71]. However, reactivity still requires time to change to a new state, which can lead to short-term service degradation and additional uncertainty at a time where unexpected things are already occurring. A more desirable approach would be to never change announcements carrying live traffic, which is known to sometimes lead to outages [6, 49, 10, 65].

Too Conservative: Another approach is to overprovision resources to handle transient peak loads [103, 1, 65]. Figure 2 demonstrates however, using longitudinal link utilization data from OVH cloud [85], that doing so can incur excessive costs. Meta also stated that solely installing extra capacity without shifting traffic is not always a feasible solution since peering capacity cannot be unilaterally upgraded [95], and Microsoft said the same because of lead time [30].

Upgrading capacity has fixed costs (*e.g.,* fiber, router backplane bandwidth, line card upgrades, CDN servers near peering routers) and variable costs (*e.g.,* power, transit), both of which scale with demand and Service Providers strive to keep low [86, 1, 15, 99]. We model deployment cost as correlated with the peering capacity over all links/sites, even though the actual relationship may be complex and additional peering capacity itself is not prohibitively expensive.

To generate Figure 2 we first split the dataset into successive, non-overlapping 120-day planning periods and compute the 95^{th} percentile ingress link utilization ("near-peak load") for each link and for each period. The dataset reports utilizations over approximately 5-minute intervals. We then simulate assigning future capacities from period to period by setting each link's capacity for the next period as the near-peak load in the current period multiplied by some overprovisioning factor (varying the factor on the X axis). We then compute the average link utilizations in the next period and the total number of links on which we see $\geq$ 100% utilization in at least one 5-minute interval.

Figure 2 plots the median utilization across links and periods and the number of congestive events as we vary the overprovisioning factor. Figure 2 shows that overprovisioning to accommodate peak loads introduces a tradeoff between inefficient utilization and overloading. Low overprovisioning factors between 10% and 30% lead to more efficient utilization (60%-70%) but lead to thousands of congestive events. High overprovisioning factors lead to far less overloading, but only roughly 50% utilization.

Efficient, Proactive Planning is Possible: Despite these limitations, Figure 1c shows that by advertising prefix 2 to

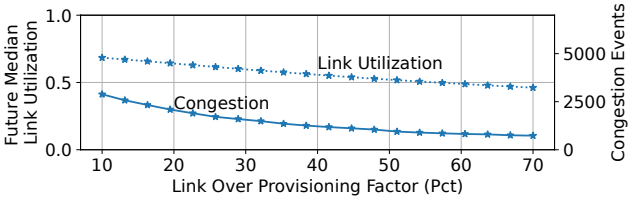

Figure 2: Planning for peak loads to avoid overloading requires inefficient overprovisioning.

provider 2 at site A a priori, the Service Provider can split traffic between the two links during failure, avoiding overloading without (a) reacting to the failure and (b) upgrading deployment capacity.

2.4 Key Challenges

Since a Service Provider has lots of global capacity, dynamically placing traffic on paths to optimize performance objectives subject to capacity constraints would therefore be simple if all the paths to the Service Provider were always available to all users as in Figure 1d. However, making paths available uses IPv4 prefixes, which are monetarily expensive and pollute BGP routing tables. The solution in Figure 1d uses 50% more prefixes than the solution in Figure 1c and, at $20k per prefix for 10,000 peerings would cost $200M [80]. IPv6 is not a good alternative, as IPv6 routing entries take 8× the amount of memory to store in a router so would pollute global routing tables even more. Prior work noted the same but found that advertising around 50 prefixes was acceptable [115, 55], and most Service Providers advertise fewer than 50 today according to RIPE RIS BGP data [101]. We also verified with engineers at six Service Providers that this challenge important to address.

Since we cannot expose all the paths by advertising a unique prefix to each connected network, we must find some subset of paths to expose.

Finding that right subset of paths to expose that satisfies performance objectives, however, is hard since there are exponentially many subsets to consider, and each subset currently needs to be tested (*i.e.,* advertised via BGP) to see how it performs. The number of subsets is on the order of 2 to the number of ingresses Service Providers have, which, for some Service Providers (including Vultr, which we measure) [105], is $> 2^{10{,}000}$. As measuring this many advertisements is intractable, we have to predict how different subsets of paths perform, which is challenging since interdomain routing is difficult to model [96, 71].

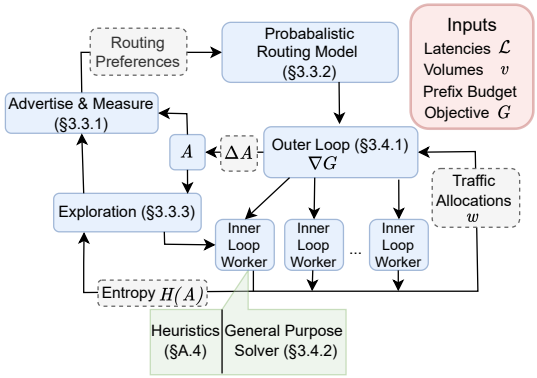

Figure 3: SCULPTOR advertisement computation overview.

3 Methodology

3.1 SCULPTOR Overview

SCULPTOR's goal is to find an advertisement strategy that gives users good interdomain paths (relative to some objective) and a traffic allocation to those paths. SCULPTOR computes BGP advertisements proactively, only placing live traffic on them after convergence. For objectives we consider, resulting optimization problems are often large with more than 100M constraints and 2M decision variables (§3.2.2). Our framework breaks this challenging problem into manageable components — Figure 3 shows the interactions among these components.

Minimizing an objective function requires evaluating it with many different inputs, but performing such measurements (*i.e.,* advertising prefixes) could take years at our problem size (§3.3.1) and so is not scalable. Instead, we estimate the objective using a "Probabilistic Routing Model" (§3.3.2) and update this model over time by "Advertising & Measuring" a small number of advertisements in the Internet, partially using entropy-based "Exploration" (§3.3.3).

We then minimize the objective function using gradient descent ("∇G") which, at each iteration, requires solving millions of sub-problems for traffic allocations ("Inner Loop Workers", §3.4.1). These sub-problems can either be solved exactly with a "General Purpose Solver" (§3.4.2) or with efficient heuristics (Appx. A.4).

3.2 Problem Setup and Definitions

3.2.1 Setting

Service Providers offer their services from tens to hundreds of geo-distributed sites [73]. The sites for a particular service can serve any user, but users benefit from reaching a low-latency site for performance. Sites consist of sets of servers that have an aggregate capacity. Sites can forward requests to other sites via private WANs as in FastRoute, but such forwarding is undesirable since it uses valuable private WAN capacity [52].

Service Providers also connect to other networks at sites via dedicated links or shared IXP fabrics which we call peering links. Each such link also has a capacity. When utilization of a site or link nears/exceeds the capacity, performance suffers, so Service Providers strive to avoid high utilization [30, 15]. Resources can also fail completely due to, for example, physical failure and misconfiguration.

Users route to the deployment through the public Internet to a prefix over one of the peering links via which that prefix is advertised. The path to a prefix (and therefore peering link) is chosen via BGP. We fix the maximum number of allowable prefixes according to the Service Provider's budget, which is generally much less than the number of peerings.

We model interdomain paths from users to the Service Provider as non-overlapping, except at the peering link through which each path ingresses to the Service Providers' deployment. We assume the peering link is the bottleneck of each path for two reasons. First, this link increasingly represents the most important part of the path for Service Providers due to Internet flattening [4]. Second, other parts of the path are less interesting from an optimization perspective—last-mile bottlenecks will be common to all paths for a `UG`, and existing systems optimize intradomain paths in other networks. Handling unexpected bottlenecks can also be viewed as an "Unseen Scenario" (§3.2.3) so `SCULPTOR` may gracefully handle violations of this assumption.

A user may have many paths to a site through different links, each with different capacities and latencies. A path to a given prefix will be through one of the corresponding ingress links over which that prefix is advertised.

We consider users at the granularity of user groups (`UG`*s*), where a `UG` refers to user networks that route to the Service Provider similarly, but could mean different things in different instantiations of our system (*e.g.,*/24 IPv4 prefixes, metros). `UG`*s* generate steady-state traffic volumes, $v_{\texttt{UG}}$, and the Service Provider provisions capacity at links/sites to accommodate this load. A system run by the Service Provider measures latency from `UG`*s* to Service Provider peering links l, which is a reasonable assumption [9, 13, 24, 34, 115, 55].

We assume that the Service Provider has some technology for directing traffic towards prefixes that `SCULPTOR` can use to direct a `UG`. Examples include DNS [98, 13, 8, 57], multipath transport [89, 22, 23], or control-points at/near user networks [92, 55]. DNS offers slow redirection due to caching [55] but is the most readily deployable by the largest number of Service Providers, whereas Service Provider-controlled appliances offer precise control but may not be a feasible option for some Service Providers. Service Providers with stronger incentives to provide the best service to users will invest in better options with more control, and eventually multipath transport will see wide enough deployment to be used by all Service Providers. Today, MPTCP is enabled by default in iOS [3] and Ubuntu 22 [31], and MPQUIC can be used in any application [117].

3.2.2 General Formulation

The problem of finding advertisement configurations that admit good assignments of user traffic to paths is a multivariate optimization over both configurations and traffic assignments.

We represent an advertisement configuration A as a binary vector. Each entry indicates whether we advertise/do not advertise a particular prefix to a particular peer/provider (similar to prior work [115, 55]). Implementing this advertisement configuration (*i.e.,* advertising prefixes via BGP sessions) results in routes from users to the Service Provider. The assignment of traffic to resulting routes from this advertisement configuration is given by the nonnegative real-valued vector w, whose entries specify traffic allocation for each user along each route.

Announcing a configuration will result in some set of routes (although knowing exactly which routes a priori is challenging), and these routes define which ingress link a `UG` uses for a prefix. We can think of this process as a routing function R that takes an advertisement configuration A and outputs a map from $\langle \texttt{prefix, UG} \rangle$ pairs to ingress links. For example, say $R(A) = f_A$, and $f_A(p, \texttt{UG}) = l$ — this notation means that the output of an advertisement configuration A under routing R is a function f_A that tells us that users `UG` reach prefix p via link l. It could be that a configuration leads to no route for some `UG` to some prefix. We define a function e such that $e(R(A)(p, \texttt{UG})) = 1$ when there is some route for `UG` to prefix p under configuration A, and 0 otherwise.

Now suppose the overall metric we want to minimize is G which is a function of both configurations and traffic assignments. Examples include traffic cost, average latency, maximum latency, and their combinations (see Appx. A.3 for a discussion of which metrics may work better than others). The joint minimization over configurations and traffic assignments can then be expressed as the following.

$$\begin{aligned} \min_{A,w} \quad & G(R(A), w) \\ \text{s.t.} \quad & w(p, \texttt{UG}) \geq 0; \quad A(p,l) \in \{0,1\} \quad \forall \texttt{UG}, p, l \\ & \sum_p w(p, \texttt{UG}) e(R(A)(p, \texttt{UG})) = v(\texttt{UG}) \quad \forall \texttt{UG} \end{aligned} \tag{1}$$

The first constraint requires that traffic assignments be nonnegative and that configurations are binary. The second constraint requires that all user traffic $v(\texttt{UG})$ is assigned, and none is assigned to nonexistent paths. Capacity constraints depend on the choice of G.

3.2.3 Specific Objectives

In our evaluations we focus on two specific objectives: (1) minimizing latency and maximum link utilization in unseen scenarios, and (2) optimally routing different traffic classes. We believe the framework will accommodate objectives that have been met in other networking settings

[99, 95, 109, 55, 115, 13, 15, 48, 37, 66], although we provide no formal characterization of which objectives definitely work (because the gradient descent approach it uses does not provide formal guarantees (Appx. A)). With our interdomain path model (§2.2), steady-state path latency for a UG to a prefix is uniquely determined by UG and the corresponding peering link over which the UG ingresses (but latency may change, which we evaluate in Section 5.2.2. Let the latency for a user UG via a link l be $\mathcal{L}(\text{UG}, l)$. G is then given by the following.

$$G(R(A), w) = \frac{1}{\sum_{\text{UG}} v(\text{UG})} \sum_{p,\text{UG}} \mathcal{L}(\text{UG}, R(A)(p, \text{UG}))w(p, \text{UG}) \; + \; \beta M$$
$$\text{s.t.} \; \frac{\sum_{R(A)(p,\text{UG})=l} w(p, \text{UG})}{c(l)} \leq M \quad \forall l \tag{2}$$

Constraining maximum link utilization, M, to be at least as much as the utilization of each link and then minimizing a sum including it forces M to be the maximum link utilization. The sum of average latency and maximum link utilization is weighted by a parameter, β, which represents a tradeoff between using uncongested links/sites and low propagation delay and is set by the Service Provider based on their goals. We first solve Equation (2) with $M = 1$ to see if we can allocate traffic to paths with zero overloading. However such overload-free solutions may not exist for all A.

Unseen Scenarios To encourage good solutions to Equation (1) not only in steady-state but also in unseen conditions (failures, shifting traffic distributions), we add a term to G given by $\sum_l \alpha_l G(R(A * F_l), w)$. The vectors F_l are binary vectors defined so that multiplying advertisements, A, by these vectors simulates withdrawal/failure on a link/site (*i.e.,* zeroing out the corresponding components). This term (*i.e.,* regularizer) intuitively encourages advertisement solutions to provide UG*s* good primary and backup paths, thus preparing for dynamic conditions. In Appendix A.2 we discuss why this regularizer helps us find a good global minimum by drawing analogies to the deep learning literature.

Different Traffic Classes To demonstrate that SCULPTOR works with other useful objectives, we consider a separate problem where we try to route traffic with different performance requirements. Service Providers already perform multi-class traffic engineering on their private WANs [37, 48] and would increasingly benefit from such capabilities in an interdomain setting due to varied service offerings (§2.1), but they currently have no capability to do so. We use a similar scenario to the private WAN setting where one traffic class (high priority) should be routed with low latency, and the other (low priority) should not congest the high priority traffic. A key additional challenge in the interdomain setting is that we cannot use priority queueing to ensure that high priority traffic is not congested since we do not control queue behavior on the path. The objective function is a weighted combination of the average latency of high priority traffic and the amount of high priority traffic that is congested. We also constrain the maximum low priority overprovisioning on any link so that not all low priority traffic lands on one link, as this solution would lead to poor low priority goodput.

3.3 Predicting Interdomain Routes

Solving Equation (1) is challenging because we need to compute $G(R(A), w)$, but measuring $R(A)$ exactly requires advertising prefixes in the Internet which can only be done infrequently to avoid route-flap-dampening. Our optimization (detailed below) requires evaluating $G(R(A), w)$ for millions of different A which could take a hundred years at a rate of advertising one strategy roughly 20 minutes - 2 hours. Hence we model, instead of measure, UG paths and improve this model over time through relatively few measurements.

3.3.1 Initialization and Measuring $R(A)$

We initialize our strategy to be anycast on one prefix, and unicast on remaining prefixes (*i.e.,* one prefix per site). If we have more prefixes in our budget, we advertise those prefixes via randomly chosen ingresses.

During optimization we measure $R(A)$ by occasionally advertising the corresponding prefixes via peerings as specified by A and measuring routes taken by UG*s* to each prefix. We alternate between measuring advertisements we think are good (§3.4) and ones we think offer useful information (§3.3.3).

3.3.2 Probabilistic UG Paths

We model the routing function, and therefore our objective functions, probabilistically and update our probabilistic model over time as we measure how UG*s* route to the deployment. When, during optimization, we require a value for $G(R(A), w)$, we compute its expected value given our current probabilistic model. We compute this expected value either approximately via Monte-Carlo methods, or exactly if G's structure admits efficient computation (Appx. A.4).

Our probabilistic model assumes a priori, for a given UG towards a given prefix, that all ingress link options that prefix is advertised to that are reachable from a UG are equally likely. (Providers can discern the set with high reliability based on which ingresses the UG is reachable from.) Upon learning that one ingress is preferred over the other, we exclude that less-preferred ingress as an option for that UG in all future calculations for all prefixes for which both ingresses are an option. Prior work used a similar routing model [115, 96, 55] but did not extend it to deal with general objectives nor did it treat routing probabilistically.

A useful property of many choices of objective function G is that we do not need to approximate the routing function perfectly to solve Equation (1). For example, most UG*s* have similar latency via their many paths to a single site [94], so

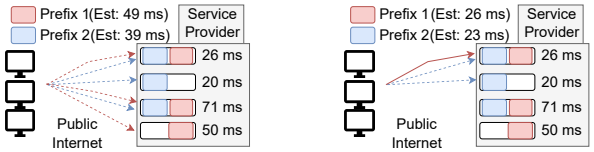

(a) (b)

Figure 4: With no knowledge of routing preferences, we estimate latency from this UG to both the red and blue prefixes with the average over possible ingress latencies (4a). A priori, no prefix is advertised. We then advertise the red prefix and measure the path towards the red prefix (*e.g.,* using `traceroute`) and learn that the first ingress has higher preference than the third and fourth ingresses (4b). We use this information to refine our latency estimate towards the blue prefix (since the third ingress is no longer a possible option) without advertising the blue prefix, saving time.

when optimizing latency as in Equation (2) we effectively only need to predict the site the user ingresses at. As we exclude more options of where UG*s* could possibly ingress for each prefix, our objective function's distribution on unmeasured scenarios converges to the true value.

An example of this process is shown in Figure 4, where we refine a latency estimate towards an unmeasured prefix (blue) using measurements towards other prefixes (red). Even though we only have 50% confidence in exactly which path the user takes (*i.e.,* in $R(A)$), we have high confidence that the user's latency towards the blue prefix will be about 23 ms.

3.3.3 Exploration to Refine $R(A)$

As, a priori, we do not know UG preferences, estimates of G could be noisy until we learn preferences. To refine our model, we periodically measure $R(A)$ on "adjacent" advertisement configurations to the configuration at the current optimization step (§3.4). By adjacent configurations, we mean configurations that differ from the current configuration, A, by one entry, or configurations representing failures ($A \times F_1$). Of the adjacent options, we select the one for which the model is most uncertain about whether it will be better or worse (*i.e.,* the probabilistic options include both). One could use various measures of uncertainty—we choose entropy. We measure adjacent configurations since we use a descent-based optimization (§3.4) which benefits from knowing whether nearby strategies are better.

3.4 A Two Pronged Approach

Even with our probabilistic model, we cannot solve Equation (1) directly/exhaustively since it is a mixed-integer program with millions of constraints which is too large for off-the-shelf solvers. Greedy [55] and random [115] approaches find good solutions in this setting for simple objectives such as steady-state latency, but, without more intelligent search through the large space, those approaches can converge to poor solutions on other objectives (§5.4).

Instead, we split Equation (1) into an outer and inner optimization, solving for configurations, A, in the outer loop using gradient descent and traffic assignments, w, in the inner loop using a general-purpose solver. Intuitively, this approach works because it breaks up a challenging optimization into many sub-problems that can be solved in parallel, and is guaranteed to push us towards *a* (perhaps locally optimal) solution.

3.4.1 Outer Loop: Gradient Descent

To apply gradient descent to our integer configuration variable, we extend A to be a continuous variable with entries between 0 and 1 and threshold its entries at 0.5 to determine if a prefix is advertised/not advertised to a certain peer/provider. We approximate gradients between adjacent advertisements by computing the expected value of $G(R(A), w)$ at each advertisement and continuously interpolate G at intermediate configurations using sigmoids (similar to prior work in a different domain [61]). We do not compute all entries of the gradient of Equation (1) since there are too many to compute. Instead, we subsample entries of the gradient and track the largest entries (similar to prior work in a different domain [97]).

Scaling: Minimization in the outer loop scales with the product of the number of ingresses and number of prefixes. Despite this high complexity, in practice the implementation runs quickly relative to our announcement rate (20-50 announcements required, 20 minutes - 2 hours per announcement). Gradient entry computations are parallelizable so this loop scales horizontally to where announcements are the key bottleneck.

Convergence: Gradient descent converges to a local minimum for bounded objectives [62]. Our evaluations show that SCULPTOR finds good solutions over a wide range of simulated topologies and converges quickly with thousands of UG*s* and ⟨`peering, prefix`⟩ pairs (§5). We comment on which problem properties will likely lead to faster convergence to more a optimal minimum in Appendix A.2 by drawing analogies to the deep learning literature. Allocating higher prefix budgets and adding richer advertisement capabilities (*e.g.,* BGP community tagging) can lead to convergence to a better minimum, which is an area for future work.

3.4.2 Inner Loop: General Purpose

Each iteration of the outer loop requires solving for traffic allocations on advertisements corresponding to the gradient entries that we wish to compute. We refer to the process of solving for these traffic allocations as an inner loop.

Scaling: In the case where we use Monte Carlo methods to approximate $G(R(A), w)$, we solve for allocations given several randomly generated $R(A)$. Hence the number of itera-

tions in the inner loop scales with the product of the number of Monte Carlo simulations and the scaling behavior of each traffic allocation, which depends on the objective.

Convergence depends on the objective, G, and the solver. The objectives we use (§3.2.3) and many others can be expressed as linear programs that are convex, so solvers can find globally optimal solutions. Useful non-convex objectives such as `Cascara`'s sometimes have approximately optimal solutions [99].

4 Implementation

We prototype `SCULPTOR` on the PEERING testbed [93], which is now available at 32 Vultr cloud sites. We describe how we built `SCULPTOR` on the real Internet and how we *emulate* a Service Provider including their clients, traffic volumes, and resource capacities. (We are not a Service Provider and so could not obtain actual volumes/capacities, but our extensive evaluations (§5) demonstrate `SCULPTOR`'s potential in an actual Service Provider and our open/reproducible methodology provides value to the community.)

4.1 Simulating Clients and Traffic Volumes

To simulate client performances, we measured actual latency from IP addresses to our PEERING prototype as in prior work [55], and selected targets according to assumptions about Vultr cloud's client base.

We first tabulate a list of 5M IPv4 targets that respond to ping via exhaustively probing each /24. Vultr informs cloud customers of which prefixes are reachable via which peers, and we use this information to tabulate a list of peers and clients reachable through those peers.

After tabulating peers, we then measure latency from all clients to each peer individually by advertising a prefix solely to that peer using Vultr's BGP action communities and pinging clients from Vultr. We also measure performance from all clients to all providers individually, as providers provide global reachability.

In our evaluations, we limit our focus to clients who had a route through at least one of Vultr's direct peers (we exclude route server peers [12]). Vultr likely peers with networks with which it exchanges a significant amount of traffic [95], so clients with routes through those peers are more likely to be "important" to Vultr. We found 700k /24s with routes through 1086 of Vultr's direct ingresses. In an effort to focus on interesting optimization cases, we removed clients whose lowest latency to Vultr was 1 ms or less, as these were assumed to be addresses related to infrastructure, leaving us with measurements from 666k /24s to 825 Vultr ingresses.

As we do not have client traffic volume data, we simulate traffic volumes in an attempt to both balance load across the deployment but also encourage some diversity in which clients have the most traffic. To simulate client traffic volumes, we first randomly choose the total traffic volume of a site as a number between 1 and 10 and then divide that volume up randomly among clients that `anycast` routes to that site. Client volumes in a site are chosen to be within one order of magnitude of each other.

Although these traffic volumes are possibly not realistic, in demonstrating the efficacy of `SCULPTOR` over a wide range of subsets of sites and simulated client traffic volumes, we demonstrate that `SCULPTOR`'s benefits are not tied to any specific choice of sites or traffic pattern within those sites.

4.2 Deployments

We use a combination of real experiments and simulations to evaluate `SCULPTOR`. Both cases use simulated client traffic volumes, but our real experiments measure real paths using RIPE Atlas probes, while our simulations use simulated paths.

We implement `SCULPTOR` with Nesterov's Accelerated Gradient Descent (§3.4.1) in Python [81]. We set $\alpha_l = 4.0$ and set the learning rate to 0.01 with decay over iterations. We solve traffic allocations (§3.4.2) with Gurobi [83].

Experiments in the Internet We assess how `SCULPTOR` performs on the Internet using RIPE Atlas probes [100], which represent a subset of all clients. RIPE Atlas allows us to measure paths (and thus ingress links) to prefixes we announce from PEERING, which `SCULPTOR` needs to refine its model (§3). However, RIPE Atlas does not have large coverage, as probes are only in 3,000 networks.

We limit the scale of our deployment to 10 large sites to avoid reaching RIPE Atlas daily probing limits (15k traceroutes/day). We choose a deployment with high site density rather than greater geographical coverage, as we believe the proximity creates a more interesting routing surface to optimize over (differences from `unicast` could be smaller, for example). These 10 sites were Miami, New York, Chicago, Dallas, Atlanta, Paris, London, Stockholm, Sao Paulo, and Madrid. We use 12 prefixes, which is low, since we do not have many prefixes. Choosing RIPE Atlas probes to maximize network coverage and geographic diversity, we select probes from 972 networks in 38 countries which have paths to 484 unique ingresses. Each probe has paths via approximately 60 ingresses.

Simulations We also evaluate `SCULPTOR` by simulating user paths which allows us to conduct more extensive evaluations, as experiments take less time and use clients in more networks. We compute solutions over many random routing preferences, demands, and subsets of sites to demonstrate that `SCULPTOR`'s benefits are not limited to a specific deployment property. We evaluate `SCULPTOR` over deployments of size 3, 5, 10, 15, 20, 25, and 32 sites. Each size deployment is run at least 10 times with random subsets of `UG`*s*, `UG` demands, and routing preferences. The distribution of the number of /24s per peer is Pareto-like, so we consider random subsets of /24s through each ingress in a way that roughly balances

the number of unique /24s per ingress. Over all scenarios, we consider paths from clients in 52k prefixes (representing 31% of APNIC population [40]) to 873 ingresses. We use one tenth of the number of ingresses as the number of prefixes in our budget. For larger deployments (20-32 sites) we use approximately 60 prefixes, and for smaller ones (3-15 sites) we use between 10 and 30. Prior work found that using this many prefixes to improve performance was a reasonable cost [115, 55].

4.3 Setting Resource Capacities

We assume that resource capacities are overprovisioned proportional to their usual load. However, we do not know the usual load of Vultr links and cannot even determine which peering link that traffic to one of our prefixes arrives on, as Vultr does not give us this information. (This limitation only exists since we are not a Service Provider, as a Service Provider could measure this using `IPFIX`, for example.) We overcome this limitation using two methods corresponding to our two deployments in Section 4.2, each with their pros and cons.

Experiments in the Internet For our first method of inferring client ingress links, we advertise prefixes into the Internet using the PEERING testbed [93], and measure actual ingress links to those prefixes using traceroutes from RIPE Atlas probes [100]. Specifically, we perform IP to AS mappings and identify the previous AS in the path to Vultr. This approach has limited evaluation coverage, as RIPE Atlas probes are only in a few thousand networks. In cases where we cannot infer the ingress link even from a traceroute, we use the closest-matching latency from the traceroute to the clients' (known) possible ingresses. For example, if an uninformative traceroute's latency was 40 ms to Vultr's Atlanta site and a client was known to have a 40 ms path through `AS1299` at that site, we would say the ingress link was `AS1299` at Atlanta.

Simulations The second method we use to infer ingress links is simulating user paths by assuming we know all user routing preference models (§3.2). We use a preference model where clients prefer peers over providers, and clients have a preferred provider. When choosing among multiple ingresses for the same peer/provider, clients prefer the lowest-latency option. We also add in random violations of the model. This second approach allows us to evaluate our model on all client networks but may not represent actual routing conditions. However, we found that our key evaluation results (§5) hold regardless of how we simulated routing conditions (we also tried completely random preference assignments), suggesting that our methodology is robust to such assumptions. Prior work also found the preference model to be valid in 90% of cases they studied [115].

Given either method of inferring client ingress links (RIPE Atlas/simulations), we then measure paths to an `anycast` prefix and assign resource capacities as some overprovisioned percentage of this catchment. (Discussions with operators from Service Providers suggested that they overprovision using this principle.) We report results for an overprovisioning rate of 30%, but find similar takeaways for 10% through 50%.

5 Evaluation

5.1 General Evaluation Setting

We compare `SCULPTOR` to other solutions.

`anycast`: A single prefix announcement to all peers/providers at all sites, which is a common strategy used by Service Providers today [33, 16, 8, 107, 87, 113, 118].

`unicast`: A single prefix announcement to all peers/providers at each site (one per site). Another common strategy used in today's deployments [98, 57, 13].

`AnyOpt/PAINTER`: Two proposed strategies for reducing steady-state latency compared to `anycast` [115, 55]. We do not compute the solution for `AnyOpt` for our evaluations on the Internet since `AnyOpt` did not perform well compared to any other solution in our simulations, and since `AnyOpt` takes a long time to compute.

`One-per-Peering`: A unique prefix advertisement to each peer/provider, so many possible paths are always available from users. This solution serves as our performance upper-bound, even though it is prohibitively expensive. (We do not know an optimal solution with fewer prefixes.)

We compute both average overall latency and the fraction of traffic within 10 ms (very little routing inefficiency), 50 ms (some routing inefficiency), and 100 ms (lots of routing inefficiency) of the `One-per-Peering` solution for each advertisement strategy, as these statistics provide a more informative measure of latency improvement than averages.

5.2 Handling Unseen Conditions

In optimizing for user latency (§3.2.3), `SCULPTOR` achieves that objective both during steady-state and also during failures and conditions unseen at the time of optimization.

For context, at the scale of Service Providers that serve trillions of requests per day, improving a few percent of traffic by tens of milliseconds represents a significant improvement. Service Providers recently emphasized that small percentage gains are important [29, 110].

5.2.1 Lower Latency in Steady-State

Internet Deployment We compute the latency that each advertisement solution achieves compared to the `One-per-Peering` solution for each `UG` on our deployment in the Internet. Figure 5a shows a CDF of the difference in latency between each solution and `One-per-Peering` for all `UG`*s*, weighted by traffic. `SCULPTOR` outperforms other solutions and is only 2.0 ms worse than (the unreasonably ex-

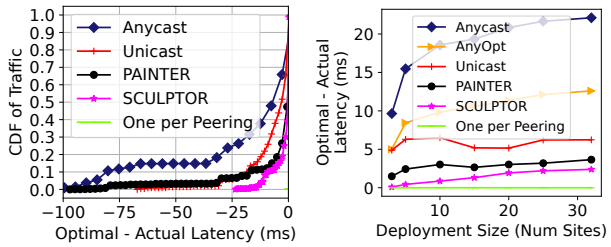

(a) (b)

Figure 5: SCULPTOR provides the lowest steady-state latency both on the Internet (5a) and in simulation (5b).

pensive) One-per-Peering solution on average, whereas the next best solution, PAINTER, is 5.5 ms worse. SCULPTOR also serves 91.8% of traffic within 10 ms of the latency with which One-per-Peering serves it, whereas the same is true for only 88% of traffic for PAINTER.

Simulations Figure 5b shows the average latency compared to the One-per-Peering solution over all simulated deployments at each deployment size. Average latency for SCULPTOR ranges from 0.1 to 2.4 ms worse than (the undeployable) One-per-Peering. The next-best solution (PAINTER) is on average 1.1 ms and 2.2 ms worse than SCULPTOR.

anycast comparatively performs the worst with UGs being on average 18.2 ms worse than One-per-Peering whereas SCULPTOR performs the best, with UGs being 1.3 ms worse than One-per-Peering. Interestingly, unicast (5.7 ms worse than One-per-Peering) actually performs better than AnyOpt (10.0 ms worse than One-per-Peering), which could be due to the different setting AnyOpt was designed for. AnyOpt was designed to optimize latency without capacity constraints over a small number of provider connections, which does not capture the realities of many Service Providers and their many peers with limited capacity [95].

These average latency improvements translate into quantifiable routing inefficiency for different fractions of traffic (we include full results in Appendix B.1). SCULPTOR has on average 94.9% traffic within 10 ms of the One-per-Peering solution, 99.2% within 50 ms, and 99.9% within 100 ms. These percentages compare favorably to the next-best solution, PAINTER, which has on average 92.3% traffic within 10 ms of the One-per-Peering solution, 97.7% within 50 ms, and 99.2% within 100 ms.

5.2.2 Better Resilience to Failure

We next assess SCULPTOR's ability to gracefully handle a type of *unseen* condition—ingress failures and site failures. Examples include excessive DDoS traffic on the link/site (thus using the link/site as a sink for the bogus traffic), physical failure, resource draining, changes in latency on a path, and planned maintenance. Figure 6 demonstrates that SCULPTOR shifts traffic without overloading alternate links/sites more effectively than any other solution, *without reactive BGP announcements/withdrawals* which could cause further failure (§2.3).

Here, we fail each ingress/site once and compute traffic allocations. For each advertisement strategy and failed component, we compute the difference between achieved latency and One-per-Peering latency for UGs that use that component in steady-state. For example, if the Tokyo site fails, we report on the post-failure latency of UGs that were served from Tokyo before the failure and not of other UGs.

In solving for traffic allocations during failure scenarios, links may be overloaded. We say all traffic arriving on a congested link is congested and do not include this traffic in latency comparisons (congested traffic latency would be a complicated function of congestion control protocols and queueing behavior). We separately note the fraction of traffic that lands on congested links and do not include it in average latency computations, but say such traffic does *not* satisfy 10 ms, 50 ms, or 100 ms objectives.

Internet Deployment Figure 6a demonstrates that SCULPTOR offers lower latency paths for more UGs during single link failure in realistic routing conditions. On average, SCULPTOR is 7.9 ms higher latency than One-per-Peering, compared to unicast which is 14.2 ms higher than One-per-Peering. PAINTER struggles to find sufficient capacity for UGs, overloading 69.6% of traffic.

Site failures (shown in Appendix B.2) show similar results. On average, SCULPTOR is 13.1 ms higher latency than One-per-Peering, while the next best solution, unicast, is 25.1 ms higher. PAINTER again performs poorly, with 95% of traffic overloaded during site failure.

Simulations We show the fraction of traffic within 50 ms of the One-per-Peering solution for link and site failures in Figure 6b and Figure 6c (further results are in Appendix B.2).

For single-link failures, anycast comparatively performs the worst with UGs being 57.9 ms worse than One-per-Peering on average, whereas SCULPTOR ranges from 0.7 ms and 9.6 ms worse than One-per-Peering on average. SCULPTOR also avoids more overloading, with only 1.3% of traffic being congested on average, while PAINTER (the next-best solution) leads to 3.7% of traffic being congested on average. Single-site failure exhibits similar trends where SCULPTOR is 8.7 ms worse than One-per-Peering's latency and has 18.5% traffic overloaded, on average, while PAINTER leads to 14.7 ms worse latency than One-per-Peering's latency and 34.8% overloading on average.

SCULPTOR also has 78.9% of traffic within 10 ms of One-per-Peering's latency on average during link failure, 93.3% within 50 ms, and 97.3% within 100 ms. The next-best solution, PAINTER, only has 66.1% within 10 ms, 81.8% within 50 ms, and 89.3% within 100 ms. Site failures show similar trends (full results are in Appendix B.2).

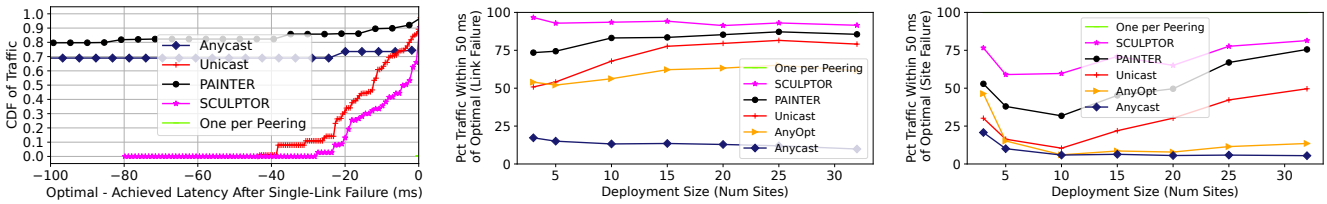

(a) (b) (c)

Figure 6: SCULPTOR improves resilience to failure both on the Internet (6a) and in simulation (6b, 6c).

5.2.3 Efficient Infrastructure Utilization

Figure 7 shows that installing more capacity to handle peak loads during unseen scenarios is not always necessary with better routing — SCULPTOR finds ways to distribute load over existing infrastructure to accommodate increased demand without adversely affecting latency. We quantify this improved infrastructure utilization under two realistic traffic patterns that SCULPTOR *did not explicitly optimize for* — flash crowds and diurnal effects.

Methodology We define a flash crowd as a transient traffic increase for users in a region. Examples of flash crowds include content releases that spur downloads in a particular region, and localized DDoS attacks. Since increased demand is localized, we can spread excess demand to other sites, which is a cheaper option than installing more capacity (see Section 3.2.1 for our cost model). We use the same provisioning model as in the rest of Section 5.2, where links are provisioned 30% higher than anycast traffic volume.

To generate Figure 7, we identify each client with a single "region" corresponding to the site at which they have the lowest possible latency ingress link. For each region individually, we then scale each client's traffic in that region by M% and compute traffic to path allocations. If there are S sites in the deployment, we thus compute S separate allocations per M value where each allocation assumes inflated traffic in exactly one region, but all the allocations are across a single set of routes calculated based on the original (non-flash) traffic. For a target region, we increase M until any link experiences overloading, then find the lowest such M value across regions. For example, if a 60% increase in traffic for Atlanta clients creates overload (and no values < 60% did for any region), we call M = 160% the critical value of M.

Our diurnal analysis in Figure 7b uses a similar methodology. We define a diurnal effect as a traffic pattern that changes volume according to the time of day. Diurnal effects might be different for different Service Providers, but a prior study from a Service Provider demonstrates that these effects can cause large differences between peak and mean site volume [15]. We sample diurnal patterns from that publication and apply them to our own traffic. We group sites in the same time zone and assign traffic in different time zones different multipliers — in "peak" time zones we assign a multiplier of M and in "trough" time zones a multiplier of $0.1M$. The full

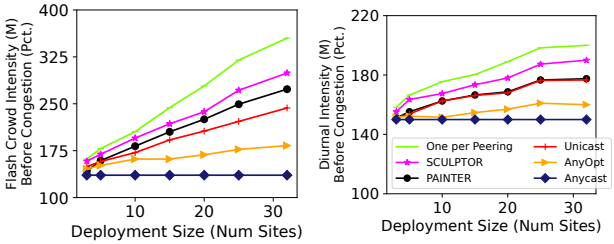

(a) (b)

Figure 7: SCULPTOR improves infrastructure utilization under flash crowds and diurnal traffic patterns so that Service Providers can underprovision compared to peak loads.

curve is shown in Appendix B.3. Similar to our flash crowd analysis, we increase M until at least one link experiences overloading at least one hour of the day.

Results Figure 7 plots the average over simulations of critical M values that cause overloading for each deployment size under flash crowds and diurnal effects computing using simulated deployments.

Figure 7a shows that SCULPTOR finds ways to route more traffic during a flash crowd without overloading than other solutions. For deployments with 32 sites, SCULPTOR can handle flash crowds at 2× more than the expected volume, creating a 3× savings in provisioning costs compared to anycast, and 26% more savings than PAINTER. Figure 7b shows that SCULPTOR also handles more intense diurnal traffic swings, allocating traffic to paths without overloading for 24% more intense swings than both PAINTER and unicast with 32 sites. Hence, instead of scaling deployment capacity to accommodate peak time-of-day traffic, Service Providers can re-distribute traffic to sites in off-peak time zones.

Moving traffic to backup paths does not necessarily mean reduced performance. SCULPTOR usually increases latency by less than 5 ms on average up to the critical M value. In practice, Service Providers can move less latency-sensitive traffic onto these backup paths so as to not impact high-level application goals. Some intradomain traffic engineering systems use similar mechanisms [48, 38, 37]. We explore this idea more thoroughly in Section 5.3.

5.3 Handling Multiple Traffic Classes

We also evaluate SCULPTOR's ability to satisfy multiple traffic classes. We split traffic into high and low priority. The objec-

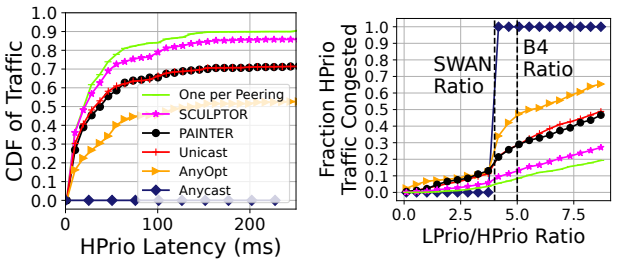

(a) (b)

Figure 8: SCULPTOR routes high priority traffic with low latency (8a) and minimal congestion from lower priority traffic (8b). We inferred LPrio/HPrio ratios for SWAN [37] and B4 [48] from those papers.

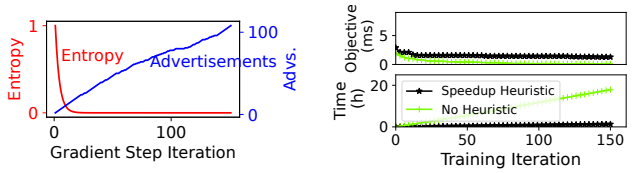

(a) (b)

Figure 9: SCULPTOR's model entropy decreases exponentially with few path measurements (9a). Heuristic speedups can also speed computation, but may sacrifice convergence (9b).

tive is to route high priority traffic to low-latency routes while limiting congestion on those routes from low priority traffic. We do not penalize cases where low priority is congested, but do limit the maximum amount of any traffic on a link to 10× the capacity of the link to avoid solutions where all low priority is placed on one link, as this solution would lead to low goodput for low priority traffic (in practice, UGs would lower sending rates in response to congestion). We solve SCULPTOR on a single simulated 32 site deployment.

In Figure 8b we vary the amount of low priority traffic as a multiple of the amount of high priority traffic and compute the fraction of high priority congestion. Links are provisioned to 5× the high priority traffic volume (different from Section 5.2), as that is roughly the LPrio/HPrio ratio reported in prior work [37, 48]. There is insufficient global capacity to route all traffic for all LPrio/HPrio over 4.0, thus the jump in anycast congestion in Figure 8b. SCULPTOR finds strategies that allow us to route more low priority traffic with less congestion than all other approaches. For example, when routing LPrio/HPrio = 5, SCULPTOR achieves half as much congestion as PAINTER and unicast.

Figure 8a also shows that SCULPTOR routes traffic with lower latency than other solutions (intercepts at the right of the graph show fractions of high priority traffic not congested). Figure 8a uses a low to high priority ratio of 4.0, a midpoint between the ratios seen in SWAN [37] and B4 [48].

5.4 Why SCULPTOR Works

Comparing More Options First, SCULPTOR compares far more advertisement strategies than the other solutions, so it has potentially better options to choose from. In our 32 site deployments, over 200 gradient steps SCULPTOR estimates latencies in approximately 20M scenarios across every UG. PAINTER only considers thousands (2k), and AnyOpt considers 1k (a configurable number, but the approach would not scale close to the numbers that SCULPTOR tries). Tango [7], a system that exposes better paths by advertising prefixes, also measures roughly thousands of different advertisements, but that system is meant for a different setting and so is not designed to scale to the complexity required of SCULPTOR.

Conducting Fewer Advertisements PAINTER has a simple method of estimating objectives in unseen scenarios which is refines through advertisements, but its greedy approach means that it only considers a single scenario per advertisement iteration. AnyOpt spends time measuring potentially uninformative advertisements. Hence, both AnyOpt and PAINTER conduct a large number of (slow to converge) advertisements on the Internet relative to the configurations they estimate, limiting the number of configurations they can explore. SCULPTOR only conducts advertisements for exploration (§3.3.3) or for strategies that SCULPTOR thinks will yield good performance (§3.4). Figure 9a shows how the maximum entropy of the distribution of G on unmeasured advertisements (§3.3.3) exponentially decreases as SCULPTOR makes these advertisements on the Internet, and so it quickly grows confident that it does not need to issue more advertisements to find good strategies. Intuitively this quick convergence manifests since we only have to predict the objective, G, not the paths (§3.3.2).

Horizontal Scaling SCULPTOR converges faster given more compute since gradient computations are parallelizable. PAINTER does not scale horizontally since it uses greedy search [55]. Some objectives additionally admit heuristics for finding approximately optimal traffic allocation solutions (*e.g.,* Appendix A.4). Other work similarly uses heuristics to quickly solve challenging optimization problems [99, 48, 84]. Figure 9b shows that our heuristic (Appendix A.4) marginally hurts SCULPTOR's convergence (2 ms average latency difference) but requires drastically less compute (50× speedup).

6 Related Work

Egress Traffic Engineering Prior work noted that traffic from Service Providers to users sometimes experienced suboptimal performance due to BGP's limitations [114, 95, 59]. SCULPTOR works in tandem with these systems, similarly working with BGP, but to optimize ingress traffic. Other work also shifts traffic to other links/sites to lower cost [116, 99, 15]. SCULPTOR adapts this idea in a new way but instead uses the public Internet to carry traffic to lower costs.

Ingress Traffic Engineering We compare SCULPTOR to other work on ingress traffic engineering [8, 67, 115, 119, 118, 71, 55] both in evaluation (§5) and discussion (§2.3). FastRoute balances users across sites to respond to chang-

ing conditions [30], but uses a private WAN to do so which is undesirable [52]. FastRoute via the public Internet would be akin to unicast, which we thoroughly compare SCULPTOR to in Section 5. PECAN [106] and Tango [7] exhaustively expose paths between endpoints and so may provide resilience to changing conditions if the right paths were exposed. However, exposing all the paths does not scale to our setting since there are too many paths to measure.

Other work and companies create overlay networks and balance load through paths in these overlay networks to satisfy latency requirements [104, 45, 2, 18, 63]. SCULPTOR can work alongside these overlay networks by advertising the external reachability of these nodes in different ways to create better paths through the overlay structure.

Prior work built a BGP playbook to mitigate DDoS attacks [91], but it is unclear if those strategies would scale to larger Service Providers (they tested on a few sites/providers). SCULPTOR deals with arbitrary unseen conditions over thousands of peering links.

Intradomain Failure Planning Service Providers have shown interest in reducing the frequency/impact of failures in their global networks [26, 35, 58, 65]. SCULPTOR works alongside these systems by, for example, enabling Service Providers to shift traffic away from failed components/regions while still retaining good performance.

Prior work also shifted traffic during peak times to limit cost/congestion [15], but did so using a private backbone. SCULPTOR's benefits are orthogonal to this prior work and useful for Service Providers without private backbones, as they use the public Internet to realize the same result.

Other prior work tried to plan intradomain routes to minimize the impact of k-component failures [109, 66, 11, 50, 15]. SCULPTOR solves different challenges that arise due to the lack of visibility/control into potential paths and their capacities in the interdomain setting.

7 Discussion & Conclusions

The control afforded to network operators in their own domains has enabled them to use new technology that improves performance, reliability, and flexibility, including fast reroute for quick recovery from failure [42], virtual routing and forwarding for flexible traffic engineering [43], and virtual output queueing for differentiated service [82]. Researchers and practitioners have proposed making similar functionality available in interdomain settings, but, after decades of little adoption, it seems unlikely that such technologies will be widespread enough for Service Providers to use them with global user populations. For example, intserv/diffserv [41] and L4S [44] are proposed frameworks for achieving differentiated service but show no signs of deployment. MIRO is a flexible interdomain multipath routing protocol that similarly shows no signs of deployment [112].

Rather than require any underlying changes to the network, SCULPTOR uses a simple, black-box model of interdomain routing, BGP's flexibility, and the unused capacity of a Service Provider's global resources to give operators power and flexibility similar to those aforementioned technologies in the interdomain setting. For example, SCULPTOR can configure multiple paths per user to enable traffic failover and can set up different routes for different traffic classes to enable virtual output queueing despite lack of control on the interdomain path. SCULPTOR is thus a step towards providing Service Providers with programmable interdomain networking primitives so that they can give us the truly resilient, low-latency network performance that our services increasingly need.

References

[1] Satyajeet Singh Ahuja, Varun Gupta, Vinayak Dangui, Soshant Bali, Abishek Gopalan, Hao Zhong, Petr Lapukhov, Yiting Xia, and Ying Zhang. [n.d.]. Capacity-efficient and uncertainty-resilient backbone network planning with hose. In *SIGCOMM 2021*.

[2] Akamai. 2022. Akamai Secure Access Service Edge. https://akamai.com/resources/akamai-secure-access-service-edge-sase

[3] Apple. 2020. Improving Network Reliability Using Multipath TCP. https://developer.apple.com/documentation/foundation/urlsessionconfiguration/improving_network_reliability_using_multipath_tcp

[4] Todd Arnold, Jia He, Weifan Jiang, Matt Calder, Italo Cunha, Vasileios Giotsas, and Ethan Katz-Bassett. [n.d.]. Cloud Provider Connectivity in the Flat Internet. In *IMC 2020*.

[5] Krishan Arora. 2023. The Gaming Industry: A Behemoth With Unprecedented Global Reach. https://forbes.com/sites/forbesagencycouncil/2023/11/17/the-gaming-industry-a-behemoth-with-unprecedented-global-reach

[6] Ann Bednarz. 2023. Global Microsoft cloud-service outage traced to rapid BGP router updates. https://networkworld.com/article/971873/global-microsoft-cloud-service-outage-traced-to-rapid-bgp-router-updates.html

[7] Henry Birge-Lee, Sophia Yoo, Benjamin Herber, Jennifer Rexford, and Maria Apostolaki. [n.d.]. {TANGO}: Secure Collaborative Route Control across the Public Internet. In *NSDI 2024*.

[8] Matt Calder, Ashley Flavel, Ethan Katz-Bassett, Ratul Mahajan, and Jitendra Padhye. [n.d.]. Analyzing the Performance of an Anycast CDN. In *IMC 2015*.

[9] Matt Calder, Ryan Gao, Manuel Schröder, Ryan Stewart, Jitendra Padhye, Ratul Mahajan, Ganesh Ananthanarayanan, and Ethan Katz-Bassett. [n.d.]. Odin: Microsoft's Scalable Fault-Tolerant CDN Measurement System. In *NSDI 2018*.

[10] Ben Cartwright-Cox. 2023. Grave flaws in BGP Error handling. https://edgecast.medium.com/the-cdn-edge-brings-compute-closer-to-where-it-is-needed-most-d4a3f4107b11

[11] Yiyang Chang, Chuan Jiang, Ashish Chandra, Sanjay Rao, and Mohit Tawarmalani. 2019. Lancet: Better network resilience by designing for pruned failure sets. (2019).

[12] Nikolaos Chatzis, Georgios Smaragdakis, Anja Feldmann, and Walter Willinger. 2013. There is more to IXPs than meets the eye. *SIGCOMM Computer Communication Review* (2013).

[13] Fangfei Chen, Ramesh K. Sitaraman, and Marcelo Torres. [n.d.]. End-User Mapping: Next Generation Request Routing for Content Delivery. In *SIGCOMM 2015*.

[14] Ping-yeh Chiang, Renkun Ni, David Yu Miller, Arpit Bansal, Jonas Geiping, Micah Goldblum, and Tom Goldstein. 2022. Loss landscapes are all you need: Neural network generalization can be explained without the implicit bias of gradient descent. In *The Eleventh International Conference on Learning Representations*.

[15] David Chou, Tianyin Xu, Kaushik Veeraraghavan, Andrew Newell, Sonia Margulis, Lin Xiao, Pol Mauri Ruiz, Justin Meza, Kiryong Ha, Shruti Padmanabha, et al. [n.d.]. Taiji: Managing Global User Traffic for Large-Scale Internet Services at the Edge. In *SOSP 2019*.

[16] Danilo Cicalese, Jordan Augé, Diana Joumblatt, Timur Friedman, and Dario Rossi. [n.d.]. Characterizing IPv4 Anycast Adoption and Deployment. In *CoNEXT 2015*.

[17] Google Cloud. 2024. Cloud Video Intelligence API. https://cloud.google.com/video-intelligence

[18] Cloudflare. 2022. Argo Smart Routing. https://cloudflare.com/products/argo-smart-routing/

[19] Cloudflare. 2024. Cloudflare Workers. https://workers.cloudflare.com/

[20] George Cybenko. 1989. Approximation by superpositions of a sigmoidal function. *Mathematics of control, signals and systems* 2, 4 (1989), 303–314.

[21] Wes Davis. 2023. Netflix ends a three-year legal dispute over Squid Game traffic. https://theverge.com/2023/9/18/23879475/netflix-squid-game-sk-broadband-partnership

[22] Quentin De Coninck and Olivier Bonaventure. [n.d.]. Multipath QUIC: Design and Evaluation. In *CoNEXT 2017*.

[23] Quentin De Coninck and Olivier Bonaventure. 2021. Multiflow QUIC: A generic multipath transport protocol. *IEEE Communications Magazine* (2021).

[24] Wouter B. De Vries, Ricardo de O. Schmidt, Wes Hardaker, John Heidemann, Pieter-Tjerk de Boer, and Aiko Pras. [n.d.]. Broad and Load-Aware Anycast Mapping with Verfploeter. In *IMC 2017*.

[25] Amogh Dhamdhere, David D Clark, Alexander Gamero-Garrido, Matthew Luckie, Ricky KP Mok, Gautam Akiwate, Kabir Gogia, Vaibhav Bajpai, Alex C Snoeren, and Kc Claffy. 2018. Inferring persistent interdomain congestion. In *Proceedings of the 2018 Conference of the ACM Special Interest Group on Data Communication*. 1–15.

[26] John P Eason, Xueqi He, Richard Cziva, Max Noormohammadpour, Srivatsan Balasubramanian, Satyajeet Singh Ahuja, and Biao Lu. [n.d.]. Hose-based cross-layer backbone network design with Benders decomposition. In *SIGCOMM 2023*.

[27] Edgecast. 2020. The CDN Edge brings Compute closer to where it is needed most. https://edgecast.medium.com/the-cdn-edge-brings-compute-closer-to-where-it-is-needed-most-d4a3f4107b11

[28] Fastly. 2024. Fastly Compute. https://fastly.com/products/edge-compute

[29] Tobias Flach, Nandita Dukkipati, Andreas Terzis, Barath Raghavan, Neal Cardwell, Yuchung Cheng, Ankur Jain, Shuai Hao, Ethan Katz-Bassett, and Ramesh Govindan. [n.d.]. Reducing web latency: the virtue of gentle aggression. In *SIGCOMM 2013*.

[30] Ashley Flavel, Pradeepkumar Mani, David Maltz, Nick Holt, Jie Liu, Yingying Chen, and Oleg Surmachev. [n.d.]. FastRoute: A Scalable Load-Aware Anycast Routing Architecture for Modern CDNs. In *NSDI 2015*.

[31] Marten Gartner. 2022. How to setup and configure mptcp on Ubuntu. https://medium.com/high-performance-network-programming/how-to-setup-and-configure-mptcp-on-ubuntu-c423dbbf76cc

[32] Jonas Geiping, Micah Goldblum, Phillip E Pope, Michael Moeller, and Tom Goldstein. 2021. Stochastic training is not necessary for generalization. *arXiv preprint arXiv:2109.14119* (2021).

[33] Danilo Giordano, Danilo Cicalese, Alessandro Finamore, Marco Mellia, Maurizio Munafò, Diana Zeaiter Joumblatt, and Dario Rossi. [n.d.]. A First Characterization of Anycast Traffic from Passive Traces. In *TMA 2016*.

[34] Palak Goenka, Kyriakos Zarifis, Arpit Gupta, and Matt Calder. 2022. Towards client-side active measurements without application control. *SIGCOMM CCR 2022* (2022).

[35] Ramesh Govindan, Ina Minei, Mahesh Kallahalla, Bikash Koley, and Amin Vahdat. [n.d.]. Evolve or die: High-availability design principles drawn from googles network infrastructure. In *SIGCOMM 2016*.

[36] Andrew Griffin. 2024. Facebook, Instagram, Messenger down: Meta platforms suddenly stop working in huge outage. https://independent.co.uk/tech/facebook-instagram-messenger-down-not-working-latest-b2507376.html

[37] Chi-Yao Hong, Srikanth Kandula, Ratul Mahajan, Ming Zhang, Vijay Gill, Mohan Nanduri, and Roger Wattenhofer. [n.d.]. Achieving High Utilization with Software-Driven WAN. In *SIGCOMM 2013*.

[38] Chi-Yao Hong, Subhasree Mandal, Mohammad Al-Fares, Min Zhu, Richard Alimi, Chandan Bhagat, Sourabh Jain, Jay Kaimal, Shiyu Liang, Kirill Mendelev, et al. [n.d.]. B4 and After: Managing Hierarchy, Partitioning, and Asymmetry for Availability and Scale in Google's Software-Defined WAN. In *SIGCOMM 2018*.

[39] W Ronny Huang, Zeyad Emam, Micah Goldblum, Liam Fowl, Justin K Terry, Furong Huang, and Tom Goldstein. 2020. Understanding generalization through visualizations. (2020).

[40] Geoff Huston. 2014. How Big is that Network? labs.apnic.net/?p=526

[41] IETF. 2000. A Framework for Integrated Services Operation over Diffserv Networks. https://datatracker.ietf.org/doc/html/rfc2998

[42] IETF. 2005. Fast Reroute Extensions to RSVP-TE for LSP Tunnels. https://datatracker.ietf.org/doc/html/rfc4090

[43] IETF. 2006. BGP/MPLS IP Virtual Private Networks (VPNs). https://datatracker.ietf.org/doc/html/rfc4364

[44] IETF. 2023. Low Latency, Low Loss, and Scalable Throughput (L4S) Internet Service: Architecture. https://datatracker.ietf.org/doc/rfc9330/

[45] INAP. 2022. INAP Network Connectivity. https://inap.com/network/

[46] Mordor Intelligence. 2022. Network as a Service Market - Growth, Trends, COVID-19 Impact, and Forecasts. https://mordorintelligence.com/industry-reports/network-as-a-service-market-growth-trends-and-forecasts

[47] Mark Jackson. 2020. Record Internet Traffic Surge Seen by UK ISPs on Tuesday. https://ispreview.co.uk/index.php/2020/11/record-internet-traffic-surge-seen-by-some-uk-isps-on-tuesday.html

[48] Sushant Jain, Alok Kumar, Subhasree Mandal, Joon Ong, Leon Poutievski, Arjun Singh, Subbaiah Venkata, Jim Wanderer, Junlan Zhou, Min Zhu, et al. [n.d.]. B4: Experience with a Globally-Deployed Software Defined WAN. In *SIGCOMM 2013*.

[49] Santosh Janardhan. 2021. More details about the October 4 outage. https://engineering.fb.com/2021/10/05/networking-traffic/outage-details/

[50] Chuan Jiang, Sanjay Rao, and Mohit Tawarmalani. [n.d.]. PCF: provably resilient flexible routing. In *SIGCOMM 2020*.

[51] Yuchen Jin, Sundararajan Renganathan, Ganesh Ananthanarayanan, Junchen Jiang, Venkata N Padmanabhan, Manuel Schroder, Matt Calder, and Arvind Krishnamurthy. [n.d.]. Zooming in on wide-area latencies to a global cloud provider. In *SIGCOMM 2019*.

[52] Bhaskar Kataria, Palak LNU, Rahul Bothra, Rohan Gandhi, Debopam Bhattacherjee, Venkata N Padmanabhan, Irena Atov, Sriraam Ramakrishnan, Somesh Chaturmohta, Chakri Kotipalli, et al. 2024. Saving Private WAN: Using Internet Paths to Offload WAN Traffic in Conferencing Services. *arXiv preprint arXiv:2407.02037* (2024).

[53] Diederik P Kingma and Jimmy Ba. 2014. Adam: A method for stochastic optimization. *arXiv preprint arXiv:1412.6980* (2014).

[54] Thomas Koch, Ethan Katz-Bassett, John Heidemann, Matt Calder, Calvin Ardi, and Ke Li. [n.d.]. Anycast in Context: A Tale of Two Systems. In *SIGCOMM 2021*.

[55] Thomas Koch, Shuyue Yu, Ethan Katz-Bassett, Ryan Beckett, and Sharad Agarwal. [n.d.]. PAINTER: Ingress Traffic Engineering and Routing for Enterprise Cloud Networks. In *SIGCOMM 2023*.

[56] Sam Kottler. 2018. February 28th DDoS Incident Report. https://github.blog/2018-03-01-ddos-incident-report/

[57] Rupa Krishnan, Harsha V. Madhyastha, Sridhar Srinivasan, Sushant Jain, Arvind Krishnamurthy, Thomas Anderson, and Jie Gao. [n.d.]. Moving Beyond End-to-End Path Information to Optimize CDN Performance. In *IMC 2009*.

[58] Umesh Krishnaswamy, Rachee Singh, Nikolaj Bjørner, and Himanshu Raj. [n.d.]. Decentralized cloud wide-area network traffic engineering with BLASTSHIELD. In *NSDI 2022*.

[59] Raul Landa, Lorenzo Saino, Lennert Buytenhek, and João Taveira Araújo. [n.d.]. Staying Alive: Connection Path Reselection at the Edge. In *NSDI 2021*.

[60] Martyn Landi. 2023. Return of original Fortnite map causes record traffic on Virgin Media O2 network. https://independent.co.uk/tech/fortnite-twitter-b2442476.html

[61] Sophie Langer. 2021. Approximating smooth functions by deep neural networks with sigmoid activation function. *Journal of Multivariate Analysis 2021* (2021).

[62] Haochuan Li, Jian Qian, Yi Tian, Alexander Rakhlin, and Ali Jadbabaie. 2024. Convex and non-convex optimization under generalized smoothness. *Advances in Neural Information Processing Systems* 36 (2024).

[63] Jinyang Li, Zhenyu Li, Ri Lu, Kai Xiao, Songlin Li, Jufeng Chen, Jingyu Yang, Chunli Zong, Aiyun Chen, Qinghua Wu, et al. [n.d.]. Livenet: a low-latency video transport network for large-scale live streaming. In *SIGCOMM 2022*.

[64] Zhihao Li, Dave Levin, Neil Spring, and Bobby Bhattacharjee. [n.d.]. Internet Anycast: Performance, Problems, & Potential. In *SIGCOMM 2018*.

[65] Bingzhe Liu, Colin Scott, Mukarram Tariq, Andrew Ferguson, Phillipa Gill, Richard Alimi, Omid Alipourfard, Deepak Arulkannan, Virginia Jean Beauregard, Patrick Conner, et al. [n.d.]. CAPA: An Architecture For Operating Cluster Networks With High Availability. In *NSDI 2024*.

[66] Hongqiang Harry Liu, Srikanth Kandula, Ratul Mahajan, Ming Zhang, and David Gelernter. [n.d.]. Traffic engineering with forward fault correction. In *SIGCOMM 2014*.

[67] Hongqiang Harry Liu, Raajay Viswanathan, Matt Calder, Aditya Akella, Ratul Mahajan, Jitendra Padhye, and Ming Zhang. [n.d.]. Efficiently Delivering Online Services over Integrated Infrastructure. In *NSDI 2016*.

[68] Sanae Lotfi, Marc Finzi, Sanyam Kapoor, Andres Potapczynski, Micah Goldblum, and Andrew G Wilson. 2022. PAC-Bayes compression bounds so tight that they can explain generalization. *Advances in Neural Information Processing Systems* 35 (2022), 31459–31473.

[69] Doug Madory. 2024. GP Leak Leads to Spike of Misdirected Traffic. https://kentik.com/analysis/BGP-Routing-Leak-Leads-to-Spike-of-Misdirected-Traffic

[70] Doug Madory. 2024. Outage Notice From Microsoft. https://twitter.com/DougMadory/status/1768286812894605517

[71] Michael Markovitch, Sharad Agarwal, Rodrigo Fonseca, Ryan Beckett, Chuanji Zhang, Irena Atov, and Somesh Chaturmohta. [n.d.]. TIPSY: Predicting Where Traffic Will Ingress a WAN. In *SIGCOMM 2022*.

[72] Congcong Miao, Zhizhen Zhong, Yunming Xiao, Feng Yang, Senkuo Zhang, Yinan Jiang, Zizhuo Bai, Chaodong Lu, Jingyi Geng, Zekun He, et al. 2024. MegaTE: Extending WAN Traffic Engineering to Millions of Endpoints in Virtualized Cloud. (2024).

[73] Microsoft. 2023. Microsoft Datacenters. https://datacenters.microsoft.com/

[74] Microsoft. 2024. Emirates Global Aluminiium cuts cost of manufacturing AI by 86 percent with the introduction of Azure Stack HCL. https://customers.microsoft.com/en-us/story/1777264680029793974-ega-azure-arc-discrete-manufacturing-en-united-arab-emirates

[75] Jeffrey C Mogul, Rebecca Isaacs, and Brent Welch. [n.d.]. Thinking about availability in large service infrastructures. In *HotOS 2017*.

[76] Nitinder Mohan, Lorenzo Corneo, Aleksandr Zavodovski, Suzan Bayhan, Walter Wong, and Jussi Kangasharju. [n.d.]. Pruning Edge Research With Latency Shears. In *HotNets 2020*.

[77] Scott Moritz. 2021. Internet Traffic Surge Triggers Massive Outage on East Coast. https://bloomberg.com/news/articles/2021-01-26/internet-outage-hits-broad-swath-of-eastern-u-s-customers

[78] Giovane CM Moura, John Heidemann, Moritz Müller, Ricardo de O. Schmidt, and Marco Davids. [n.d.]. When the dike breaks: Dissecting DNS defenses during DDoS. In *IMC 2018*.

[79] Giovane C. M. Moura, Ricardo de Oliveira Schmidt, John Heidemann, Wouter B. de Vries, Moritz Muller, Lan Wei, and Cristian Hesselman. [n.d.]. Anycast vs. DDoS: Evaluating the November 2015 Root DNS Event. In *IMC 2016*.

[80] NANOG. 2022. Panel: Buying and Selling IPv4 Addresses. https://youtube.com/watch?v=8FlTJEct9_s

[81] Yurii Nesterov et al. 2018. *Lectures on convex optimization*. Vol. 137. Springer.

[82] Juniper Networks. 2023. Understanding CoS Virtual Output Queues (VOQs). https://juniper.net/documentation/us/en/software/junos/traffic-mgmt-qfx/topics/concept/cos-qfx-series-voq-understanding.html

[83] Gurobi Optimization. 2024. Gurobi Optimizer. https://www.gurobi.com/downloads/

[84] Yarin Perry, Felipe Vieira Frujeri, Chaim Hoch, Srikanth Kandula, Ishai Menache, Michael Schapira, and Aviv Tamar. [n.d.]. DOTE: Rethinking (Predictive) WAN Traffic Engineering. In *NSDI 2023*.

[85] Maxime Piraux, Louis Navarre, Nicolas Rybowski, Olivier Bonaventure, and Benoit Donnet. [n.d.]. Revealing the evolution of a cloud provider through its network weather map. In *IMC 2022*.

[86] Leon Poutievski, Omid Mashayekhi, Joon Ong, Arjun Singh, Mukarram Tariq, Rui Wang, Jianan Zhang, Virginia Beauregard, Patrick Conner, Steve Gribble, et al. [n.d.]. Jupiter evolving: transforming google's datacenter network via optical circuit switches and software-defined networking. In *SIGCOMM 2022*.

[87] Matthew Prince. 2013. Load Balancing without Load Balancers. https://blog.cloudflare.com/cloudflares-architecture-eliminating-single-p/

[88] Matthew Prince. 2013. The DDoS That Knocked Spamhaus Offline (And How We Mitigated It). https://blog.cloudflare.com/the-ddos-that-knocked-spamhaus-offline-and-ho

[89] Costin Raiciu, Christoph Paasch, Sebastien Barre, Alan Ford, Michio Honda, Fabien Duchene, Olivier Bonaventure, and Mark Handley. [n.d.]. How Hard Can It Be? Designing and Implementing a Deployable Multipath TCP. In *NSDI 2012*.

[90] Duncan Riley. 2023. Internet's rapid growth faces challenges amid rising denial-of-service attacks. https://siliconangle.com/2023/09/26/internets-rapid-growth-faces-challenges-amid-rising-ddos-attacks

[91] ASM Rizvi, Leandro Bertholdo, João Ceron, and John Heidemann. [n.d.]. Anycast Agility: Network Playbooks to Fight DDoS. In *USENIX Security Symposium 2022*.

[92] Patrick Sattler, Juliane Aulbach, Johannes Zirngibl, and Georg Carle. [n.d.]. Towards a Tectonic Traffic Shift? Investigating Apple's New Relay Network. In *IMC 2022*.

[93] Brandon Schlinker, Todd Arnold, Italo Cunha, and Ethan Katz-Bassett. [n.d.]. PEERING: Virtualizing BGP at the Edge for Research. In *CoNEXT 2019*.

[94] Brandon Schlinker, Italo Cunha, Yi-Ching Chiu, Srikanth Sundaresan, and Ethan Katz-Bassett. [n.d.]. Internet Performance from Facebook's Edge. In *IMC 2019*.

[95] Brandon Schlinker, Hyojeong Kim, Timothy Cui, Ethan Katz-Bassett, Harsha V. Madhyastha, Italo Cunha, James Quinn, Saif Hasan, Petr Lapukhov, and Hongyi Zeng. [n.d.]. Engineering Egress with Edge Fabric: Steering Oceans of Content to the World. In *SIGCOMM 2017*.

[96] Pavlos Sermpezis and Vasileios Kotronis. 2019. Inferring catchment in internet routing. (2019).

[97] Yoav Shechtman, Amir Beck, and Yonina C Eldar. 2014. GESPAR: Efficient phase retrieval of sparse signals. *IEEE transactions on signal processing* (2014).

[98] Patrick Shuff. [n.d.]. Building a Billion User Load Balancer. https://usenix.org/conference/lisa16/conference-program/presentation/shuff

[99] Rachee Singh, Sharad Agarwal, Matt Calder, and Paramvir Bahl. [n.d.]. Cost-Effective Cloud Edge Traffic Engineering with Cascara. In *NSDI 2021*.

[100] RIPE NCC Staff. 2015. RIPE Atlas: A Global Internet Measurement Network. *Internet Protocol Journal* (2015).

[101] RIPE NCC Staff. 2023. RIS Live. (2023). https://ris-live.ripe.net

[102] Jan-Philipp Stauffert, Florian Niebling, and Marc Erich Latoschik. 2018. Effects of latency jitter on simulator sickness in a search task. In *2018 IEEE conference on virtual reality and 3D user interfaces (VR)*.

[103] Chris Stokel-Walker. 2021. Case study: How Akamai weathered a surge in capacity growth. https://increment.com/reliability/akamai-capacity-growth-surge/

[104] Subspace. 2022. Optimize Your Network on Subspace. https://subspace.com/solutions/reduce-internet-latency

[105] Ticiane Takami. 2021. Project Myriagon: Cloudflare Passes 10,000 Connected Networks. https://blog.cloudflare.com/10000-networks-and-beyond/

[106] Vytautas Valancius, Bharath Ravi, Nick Feamster, and Alex C Snoeren. [n.d.]. Quantifying the Benefits of Joint Content and Network Routing. In *SIGMETRICS 2013*.

[107] Verizon. 2020. Edgecast. https://verizondigitalmedia.com/media-platform/delivery/network/

[108] VULTR. 2023. VULTR Cloud. https://vultr.com/

[109] Ye Wang, Hao Wang, Ajay Mahimkar, Richard Alimi, Yin Zhang, Lili Qiu, and Yang Richard Yang. [n.d.]. R3: resilient routing reconfiguration. In *SIGCOMM 2010*.

[110] David Wetherall, Abdul Kabbani, Van Jacobson, Jim Winget, Yuchung Cheng, Charles B Morrey III, Uma Moravapalle, Phillipa Gill, Steven Knight, and Amin Vahdat. [n.d.]. Improving Network Availability with Protective ReRoute. In *SIGCOMM 2023*.

[111] Matthias Wichtlhuber, Eric Strehle, Daniel Kopp, Lars Prepens, Stefan Stegmueller, Alina Rubina, Christoph Dietzel, and Oliver Hohlfeld. 2022. IXP scrubber: learning from blackholing traffic for ML-driven DDoS detection at scale. In *Proceedings of the ACM SIGCOMM 2022 Conference*. 707–722.

[112] Wen Xu and Jennifer Rexford. [n.d.]. MIRO: Multi-Path Interdomain Routing. In *SIGCOMM 2006*.

[113] Jing'an Xue, Weizhen Dang, Haibo Wang, Jilong Wang, and Hui Wang. [n.d.]. Evaluating Performance and Inefficient Routing of an Anycast CDN. In *International Symposium on Quality of Service 2019*.

[114] Kok-Kiong Yap, Murtaza Motiwala, Jeremy Rahe, Steve Padgett, Matthew Holliman, Gary Baldus, Marcus Hines, Taeeun Kim, Ashok Narayanan, Ankur Jain, et al. [n.d.]. Taking the Edge off with Espresso: Scale, Reliability and Programmability for Global Internet Peering. In *SIGCOMM 2017*.

[115] Xiao Zhang, Tanmoy Sen, Zheyuan Zhang, Tim April, Balakrishnan Chandrasekaran, David Choffnes, Bruce M. Maggs, Haiying Shen, Ramesh K. Sitaraman, and Xiaowei Yang. [n.d.]. AnyOpt: Predicting and Optimizing IP Anycast Performance. In *SIGCOMM 2021*.

[116] Zheng Zhang, Ming Zhang, Albert G. Greenberg, Y. Charlie Hu, Ratul Mahajan, and Blaine Christian. [n.d.]. Optimizing Cost and Performance in Online Service Provider Networks. In *NSDI 2010*.

[117] Zhilong Zheng, Yunfei Ma, Yanmei Liu, Furong Yang, Zhenyu Li, Yuanbo Zhang, Jiuhai Zhang, Wei Shi, Wentao Chen, Ding Li, et al. [n.d.]. Xlink: QoE-Driven Multi-Path QUIC Transport in Large-Scale Video Services. In *SIGCOMM 2021*.

[118] Minyuan Zhou, Xiao Zhang, Shuai Hao, Xiaowei Yang, Jiaqi Zheng, Guihai Chen, and Wanchun Dou. [n.d.]. Regional IP Anycast: Deployments, Performance, and Potentials. In *SIGCOMM 2023*.

[119] Jiangchen Zhu, Kevin Vermeulen, Italo Cunha, Ethan Katz-Bassett, and Matt Calder. [n.d.]. The Best of Both Worlds: High Availability CDN Routing Without Compromising Control. In *IMC 2022*.

A Optimization Extensions

In our evaluations we focused on two specific objectives (§3.2.3) It could be, however, that Service Providers wish to optimize other/additional metrics. Here we try to determine which metrics our framework will more likely work for and, in doing so, identify what about SCULPTOR gives good performance. We do not provide any theoretical guarantees but give valuable intuitions.

Our high-level finding is that SCULPTOR works with most metrics we could think of, and will work better both with more prefixes and with richer BGP configurations. However, we also find that considering metrics other than latency could introduce considerable computational costs. SCULPTOR's ability to handle many different traffic conditions likely stems from its consideration of single component failures directly in the loss function.

A.1 Gradient Descent Challenges

We propose using gradient descent to solve Equation (1) because of its parallelizability which is important given the large problem sizes we consider and the complexity of predicting routes. Recent work suggests that gradient descent may not be important for finding good minimizers [14], so other minimizers may also work well for SCULPTOR.

To use gradient descent to solve Equation (1), we require that our objective function is a differentiable function of real variables. Ours, as we have presented it, does not satisfy that condition. Ignoring possible problems with the objective function G, there are two problems: first, our configuration A is a binary variable, and, second, the function R is not well-behaved.

To see what we mean by this second point, consider computing a gradient near a configuration that only advertises one prefix to one provider. A "small" change in the configuration (withdrawing that prefix) would lead to zero reachability and thus no solution, which suggests that R is not "differentiable", or at least not differentiable everywhere. Gradient descent converges to a minimum for functions whose second derivatives are locally bounded [62]. Intuitively, this condition means that a gradient should not push the descent in significantly different directions in small regions since descent could, for example, oscillate and never decrease the loss.

To solve the first problem, we apply gradient descent to continuous extensions of configurations and the routing function. There are many ways of performing this extension. One way of continuously extending these ideas that we found works well is to treat configuration components as real-valued, rather than binary, variables between 0 and 1 and interpolate objective function values between "adjacent" components of configurations using sigmoids (see Section 3 for details). Sigmoids likely work well since their configurable parameter controls steepness, which allows us to control the magnitude of gradients (*i.e.,* not making them too large which could harm convergence).

To solve the second problem, we restrict gradient descent to a region of configurations for which it is unlikely that catastrophic behavior occurs. For example, anycast configurations generally still provide (possibly congested) routes for all users when any one link fails, and so we would not expect divergence for any configuration "near" an anycast one. In practice, this restriction generally means we pick an initialization where users have paths to many links/sites, and we heavily discourage routeless configurations during gradient descent by assigning these divergent cases a large value.

This solution is reasonable as Service Providers often connect to several transit providers at each site to provide global reachability to all users even under partial congestion or failure [4].

A.2 The Key Challenge: Convergence

With bounded second derivatives of the objective function gradient descent converges to *a* minimum [62], and can converge to that minimum quickly with good initializations and choices of the learning rate. However, unless the objective function is convex (ours is not because the routing function is not) then gradient descent may converge to a local minimum. We find that SCULPTOR likely converges to a good minimum because of our choice of loss function and that this convergence could improve with more prefixes and richer BGP configuration options.

A.2.1 Nonconvexity in Deep Learning

We first draw an analogy to the Deep Learning setting which has used gradient descent with lots of success, despite its exclusive focus on nonconvex objectives. Deep Learning practitioners identified that we can think of the convergence problem in terms of both the representational power of our models and in terms of the size of our training data set.

Deep Learning tries to find functions f_α parameterized by parameters α that minimize the expectation of a loss function, where the expectation is taken over the distribution of "data". Functions f_α accept this data as input. The loss function is usually chosen so that minimizing the expected value of the loss function over parameters α results in a "useful" thing — evaluating the function f_α with learned parameters α accomplishes a useful task, such as image classification.

In practical settings we only have a corpus of data, rather than the distribution, which serve as samples of that distribution. During gradient descent, deep learning algorithms randomly sample from this corpus and move the parameter gradient roughly along the average of the gradients evaluated at each corpus point [53]. Hence, we often call gradient descent in this setting *stochastic* gradient descent. It is up for debate whether this stochasticity is an important contributor to deep learning's success [32] (or gradient descent at all [14]).

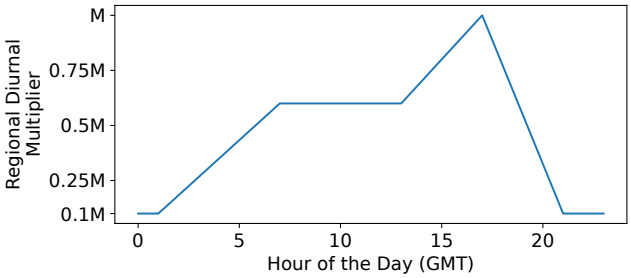

Figure 10: The diurnal traffic shape we apply in Section 5.2.3, taken from prior work [15].

Functions f_α contain potentially billions of parameters and are generally nonconvex. The functions can be compositions of many (tens to hundreds) of functions and so may be "deep". Since these functions contain so many parameters, they can both theoretically and experimentally find a global minimizer of the loss [20], despite nonconvexity. One risk of using too many parameters, however, is "overfitting" — even though a learned function f_α minimizes loss on the corpus of data, it may have high loss on unseen data. This problem is of practical importance since it is often impossible to represent every single function input with a finite data corpus. While it is generally believed that using too many parameters leads to overfitting, recent work suggests that it may relate closer to the geometry of the loss function [14].

Given a task to complete, training a deep learning model to accomplish this task consists of choosing a model, loss function, and optimization method (*e.g.,* gradient descent). To test the efficacy of a training methodology, practitioners mimic applying their learned model to a new setting by splitting their corpus into a *train* and *test* set. Practitioners then optimize using the training set, and evaluate the performance of their learned model on the test set. If practitioners observe good test performance, they can be more confident that in other settings their algorithms did not overfit and hence "generalize".

A.2.2 Nonconvexity in SCULPTOR

In our setting, the parameters α are the configuration and traffic assignment variables, since those are the variables we update with gradient descent. Our data corpus consists of path/deployment metrics (*e.g.,* latency), link capacities, and traffic volumes.

Overfitting & Generalization A potential problem with converging to a local minimum is overfitting. Our deep learning analogy identifies our training data set as both steady-state conditions and conditions under single link and site failures. We explicitly "test" SCULPTOR on flash crowds and diurnal traffic patterns (§5.2.3) and find good generalization. The question is: why does SCULPTOR provide good generalization?

Although the question of why neural networks offer generalization is open, one compelling theory relates to the geometry of the loss landscape. Prior work observes that "wide" loss regions generalize much better than thin/sharp loss regions [39]. One way of interpreting wideness is that perturbations in the parameters, α, do not significantly increase the value of the loss.

One reason why SCULPTOR might provide good generalization is that our choice of loss function encourages finding configurations that are resilient to minor changes. For example, consider a small change in the configuration that withdraws an advertisement of a specific prefix via a specific ingress. Under this change, users will have strictly more routes to the deployment than if all prefixes via that ingress were withdrawn (*i.e.,* a link failure). Hence, the feasible set of all traffic assignments, w, under single-prefix withdrawal is a superset of those assignments under the corresponding link failure, and so the optimal loss value under this small change is less than (*i.e.,* more optimal) than in the link failure setting.

Similarly, small changes in the configuration that *advertise* a prefix via specific ingress can lead to some routes to that prefix no longer being available for some UG*s* if that newly advertised ingress is preferred over others. Hence, such changes are equivalent to withdrawing the advertisement via that ingress for those UG*s*, so our above discussion still applies.

By explicitly minimizing loss under all link failures, SCULPTOR upper bounds the impact of these minor configuration variations, and so (at least intuitively) settles in a "wide" minimum.

Some objectives may also naturally provide wide a minimum in the interdomain path optimization setting we consider. For example, we observed that many UG*s* have similar latencies via many different ingresses to the same site. Hence, small changes in the traffic allocation (which is another one of our "parameters"), α may not affect the overall objective (average latency) that much if those small changes simply shift UG*s* among those different paths to the same site.

Underfitting Another concern with convergence to a local minimum is that the objective function value at that point will be much higher than it could otherwise be at the global minimum. For example, when minimizing average latency it could be that a solution to achieve 35 ms average latency exists, but gradient descent arrives at a local minimum giving an average latency of, for example, 50 ms. In Deep Learning, this problem is called underfitting and can happen when the chosen function does not have sufficient representational complexity [68].

SCULPTOR underfits the training data as shown by the suboptimality compared to the One-per-Peering solution (§5.2.2).

One way of fitting the data better is to consider richer functions with more parameters. In our setting, this option means increasing the number of "parameters" in both advertisement configurations and path options. In other words, this option

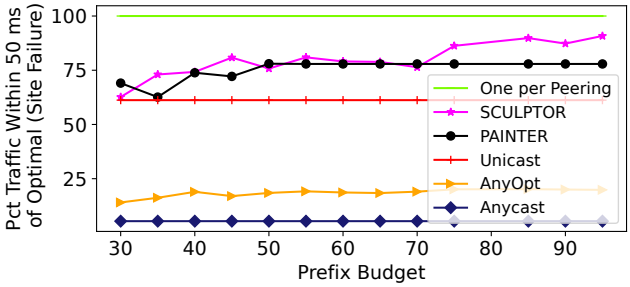

Figure 11: Using more prefixes allows SCULPTOR to converge to better solutions.

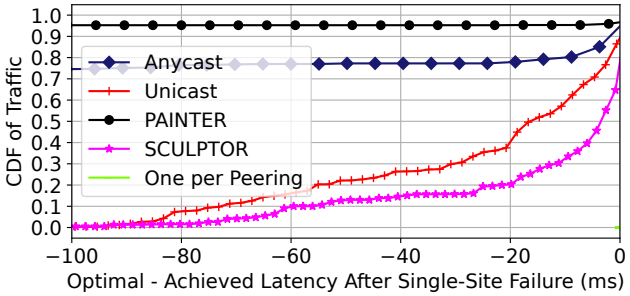

Figure 12: Our prototype on the public Internet shows that SCULPTOR offers low latency backup paths to users during site failures.

means increasing the number of prefixes, or types of configurations to offer UGs more paths. By this last point we mean, for example, using AS path prepending to potentially offer richer path options. Our investigation in Figure 11 confirms this intuition, as using more prefixes allowed us to converge to better solutions whereas using too few prefixes led to similar/worse performing configurations than PAINTER. Other work has used richer configurations to solve problems [106, 7], but adopting such methods to SCULPTOR would require solving scalability challenges.

We Do/Should Not Learn Routing with GD Another type of "learning" we discuss in Section 3 is refining our estimate of the routing function R. However, this is not descent based learning and is independent of this discussion. In Section 3 we model the function R as a random function, but one that follows a specific structure (preference routing model), and opportunistically removes randomness using Internet measurements. As we demonstrate in Figure 9a, the randomness is essentially zero for most gradient descent iterations.

We choose this approach over modeling R as in the deep learning setting since learning R requires advertising configurations in the Internet, which takes a long time. Using the known structure of R allowed for easier debugging than using blackbox deep learning models which is important given the slow iteration process.

A.3 So, Which Metrics Work?

The above challenges, solutions, and intuitions are valid independent of the specific metric we care to optimize. Certain metrics could introduce either convergence or computational challenges. Before discussing those challenges, we first present choices of G other than the ones we evaluated (§3.2.3).

A.3.1 Possible Metric Choices

Any Function of Latency: Configuring routes that minimize any function of latency are trivial extensions of objectives we considered. The objective function would take the form $G(R(A),w) = \sum_{p,\text{UG}} L(R(A)(p,\text{UG}))w(p,\text{UG})$ where the function L is some arbitrary mapping on latency. The resulting problem is a linear program in w and hence convex in w. A simple variation is maximizing the amount of traffic below a latency threshold, which may be useful for enabling specific applications [76].

Transit Cost: Configuring routes that reduce expected transit cost would roughly amount to minimizing the *maximum* traffic allocation on any provider (possibly weighted by that provider's rate, possibly only considering certain traffic). Hence the objective function would take the form $G(R(A),w) = \max_l \sum_{p,\text{UG}:G(R(A)(\text{UG},p)=l)} w(p,\text{UG})$ which can be expressed as a linear program in w. One could alternatively use methods from prior work in SCULPTOR [99].

Compute/WAN Costs: It could be that sending traffic to a certain site causes increased utilization of WAN bandwidth, compute, or power in a certain region, and that this cost scales non-linearly. Operators can specify custom cost as a function of site traffic. The objective function would take the form $G(R(A),w) = \sum_{p,\text{UG}} C(w(p,\text{UG}))$ where C is some cost function on traffic. Examples include polynomials and exponents which may not be convex in w but can still often be solved with descent-based methods (see the following subsection).

End-to-End Considerations: It could be that, for example, a particular site has low ingress latency for a UG but large egress latency and so may not be a good choice for that UG. As Service Providers have knowledge of these limitations (for example, they can measure egress link utilization or egress latency [95]), they can serve these variables as inputs into SCULPTOR and solve for path allocations, w subject to those variables.

A.3.2 Convergence Concerns

We expect functions G whose gradients do not explode in the region of interest to converge well. For configurations, A, we encourage gradients to be well-behaved with a good initialization (§3.3.1, Appx. A.1). For traffic assignments w, it depends on how the metric, G, incorporates w.

Examples of metrics G of w that offer good convergence include low-order polynomials and exponents (within a reasonable range such that gradients are not too large) whereas bad choices are ones with ill-behaved gradients. As an example, we compared convergence between $G(R(A),w) =$

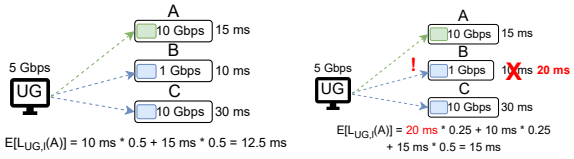

(a) (b)

Figure 13: A UG has a path to two prefixes, green and blue. The green prefix is only advertised via ingress A and the blue prefix is advertised via two ingresses B and C, each of which are equally likely for this UG. If the UG prefers B over C, we assign the client to the blue prefix (10 ms) while if the UG prefers C over B we will assign the client to the green prefix (15 ms). Hence the initial expected latency is the average of 10 ms and 15 ms corresponding to whether this UG prefers ingress B or C (13a). However, ingress B does not have sufficient capacity to handle this UG's traffic and so is congested with 50% probability corresponding to the 50% probability that this user prefers ingress B. We artificially inflate this UG's expected latency (and all other UG's using ingress B) to reflect this possible overutilization (13b).

$\sum_{p,\text{UG}} w(p,\text{UG})^2$ and $G(R(A),w) = \sum_{p,\text{UG}} \sqrt{w(p,\text{UG})}$. The latter has exploding gradients near 0 (which many values of w take on) and so SCULPTOR struggled to find a good solution, while it found a good solution for the first one. (We could not think of why a Service Provider would choose either metric, but they are possible choices.)

A.4 Heuristics for Fast Computation

With sufficient resources, solving Equation (1) using the two pronged approach outlined in Section 3.4 is feasible. Given our advertisement rate limitations (§3.3.1) we wish to compute gradients in tens of minutes. With 100 Monte Carlo simulations per gradient and tens of thousands of gradients to compute, we thus need to solve millions of linear programs at each gradient step. Meta recently demonstrated that they could solve millions of linear programs in minutes using their infrastructure [26].

As we do not have these resources, we instead use efficient heuristics to approximately solve each linear program. Our heuristics depend on the structure of our objective function, and so are specific to our choice of average latency (Eq. (2)). During optimization we observed that these heuristics tended to yield accurate estimates for G despite inaccuracies in predicting any individual UG's latency or link's utilization.

A.4.1 Capacity-Free UG Latency Calculation

Minimizers of Equation (2) balance traffic across links to satisfy capacity constraints. We instead temporarily ignore capacity constraints and assign each UG to their lowest-latency path. This approximation solves two problems at once. First, we do not need to solve a linear program to compute traffic assignments. Second, we can now analytically compute the distribution of our objective function, G, over all possible realizations of $R(A)$. Analytically computing this distribution is useful, since it lets us compute entropy (§3.3.3) and expected value (§3.3.2) without Monte Carlo methods.

To see why we can compute the distribution exactly, notice that the objective function is a composition of functions of the form $min(X,Y)$ and $X+Y$ since we choose the minimum latency path across prefixes for each UG and average these minimums. We compute UG latency distributions for each prefix exactly using our routing preference model, and use analytical methods to efficiently compute the distributions of the corresponding minimums and averages.

A.4.2 Imposing Capacity Violation Penalties

It could be that such minimum latency assignments lead to congested links. We would like to penalize such advertisement scenarios, and favor those that distribute load more evenly without solving linear programs. Hence, before computing the expected latency, we first compute the probability that links are congested by computing the distribution of link utilizations from the distribution of UG assignments to paths. We then inflate latency for UGs on likely overutilized links.

That is, for each possible outcome of UG assignments to links, we compute link utilizations and note the probability those UGs reach each link. We then accumulate the probability a link is congested as the total probability over all possible scenarios that lead to overutilization. We discourage UGs from choosing paths that are likely congested using a heuristic — we emulate the impact of overloading by inflating latency in this calculation for UGs on those paths proportional to the overutilization factor. After emulating the effect of this overloading, we recompute the expected average UG latency *without changing UG decisions*. We do not change UG decisions as doing so could induce an infinite calculation loop if new decisions also lead to overloading. This heuristic penalizes advertisement strategies that would lead to many overutilized links if every user were to choose their lowest latency option. We show an example in Figure 13.

B Further Results

B.1 Steady-State Latency

In addition to quantifying average latency during steady-state, we also compute the fraction of traffic within 10 ms, 50 ms, and 100 ms of the One-per-Peering solution during steady-state. Figure 14 shows how SCULPTOR compares more favorably to the One-per-Peering solution than other advertisement strategies.

B.2 Latency During Link/Site Failure

We show additional evaluations of SCULPTOR during link and site failures. Figure 12 shows that SCULPTOR provides good

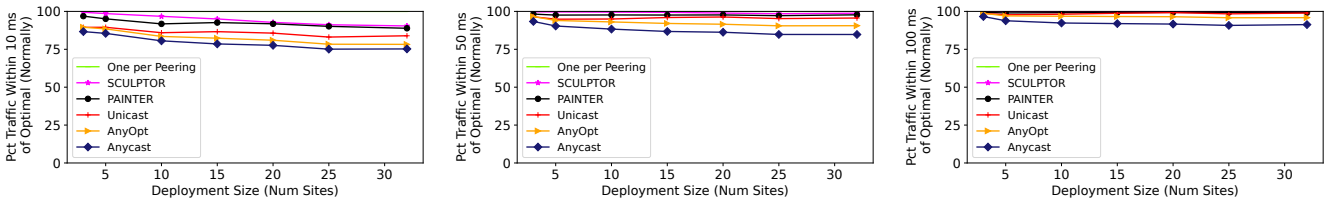

(a) (b) (c)

Figure 14: SCULPTOR lowers average latency and increases the fraction of traffic within critical thresholds of their optimal latency during normal operation.

resilience to site failures on the Internet, and Figure 15 shows similar results for link and site failures in our simulations.

B.2.1 Internet Deployment

SCULPTOR provides better resilience than other solutions to site failures on the Internet, yielding no congested traffic and on average 18.1 ms worse than One-per-Peering. The next best solution, unicast, yields 16.1% overloading and, for uncongested traffic, 28.1 ms worse latency than One-per-Peering on average.

B.2.2 Simulations

SCULPTOR provides good performance in simulation.

B.3 Infrastructure Utilization Further Results

In Figure 10 we show the shape of our diurnal curve taken from observed diurnal traffic patterns at a Service Provider [15]. We use this diurnal traffic pattern to evaluate how well balances traffic across sites (§5.2.3). Specifically, we linearly interpolate 6 points on the purple curve (Edge Node 1) in Figure 1 of that paper, capturing the essential peaks and troughs.

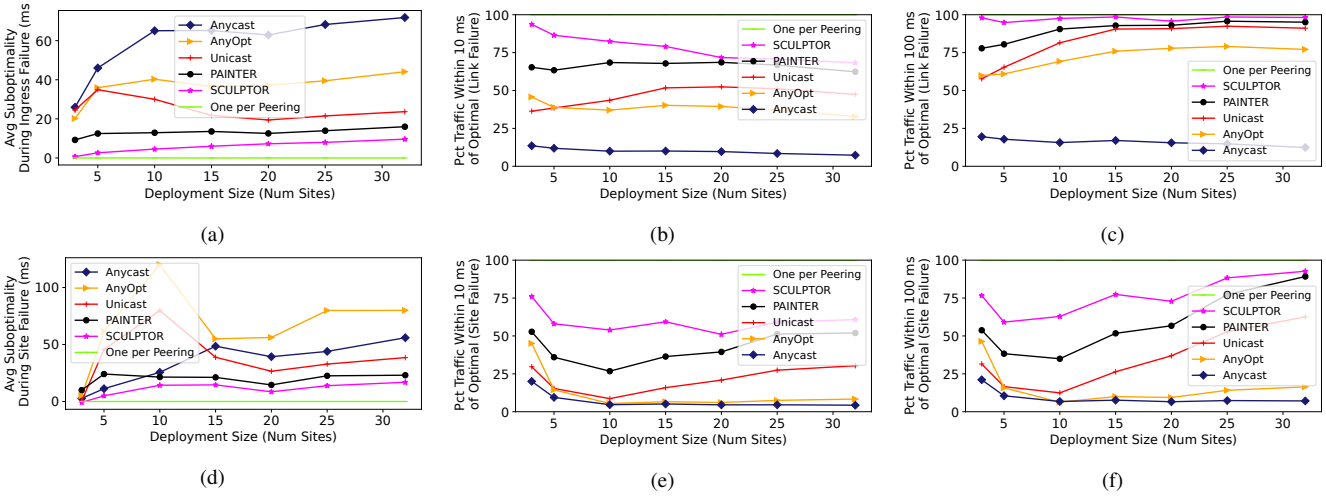

Figure 15: `SCULPTOR` lowers average latency and increases the fraction of traffic within critical thresholds of `One-per-Peering` latency during both link and site failures over many simulated deployments.